Journal of Sound and Vibration (2003) **259**(2), 265–298
doi:10.1006/jsvi.2002.5161, available online at http://www.idealibrary.com on IDEAL®

DYNAMICS BEHAVIOR OF AXISYMMETRIC AND BEAM-LIKE ANISOTROPIC CYLINDRICAL SHELLS CONVEYING FLUID

M. H. Toorani†

R&D, JDS Uniphase Corporation, Ottawa, Ontario, Canada K2G 5W8

AND

A. A. Lakis

Department of Mechanical Engineering, École Polytechnique of Montréal, Université de Montréal, C.P. 6079, Succ. Centre-ville, Montréal, Québec, Canada H3C 3A7.
E-mail:aouni.lakis@meca.polymtl.ca

(*Received* 2 *May* 2001, *and in final form* 11 *February* 2002)

The flow-induced vibration characteristics of anisotropic laminated cylindrical shells partially or completely filled with liquid or subjected to a flowing fluid are studied in this work for two cases of circumferential wave number, the axisymmetric, where $n = 0$ and the beam-like, where $n = 1$. The shear deformation effects are taken into account in this theory; therefore, the equations of motion are determined with displacements and transverse shear as independent variables. The present method is a combination of finite element analysis and refined shell theory in which the displacement functions are derived from the exact solution of refined shell equations based on orthogonal curvilinear co-ordinates. Mass and stiffness matrices are determined by precise analytical integration. A finite element is defined for the liquid in cases of potential flow that yields three forces (inertial, centrifugal and Coriolis) of moving fluid. The mass, stiffness and damping matrices due to the fluid effect are obtained by an analytical integration of the fluid pressure over the liquid element. The available solution based on Sanders' theory can also be obtained from the present theory in the limiting case of infinite stiffness in transverse shear. The natural frequencies of isotropic and anisotropic cylindrical shells that are empty, partially or completely filled with liquid as well as subjected to a flowing fluid, are given. When these results are compared with corresponding results obtained using existing theories, very good agreement is obtained.

1. INTRODUCTION

Anisotropic, laminated composite shells are increasingly used in a variety of modern engineering fields, e.g., aerospace, aeronautical, aircraft construction, nuclear and petrochemical industries. As they have a high strength- and stiffness-to-weight ratio, they offer a unique advantage compared to isotropic materials. By optimizing the properties, we can reduce the overall weight of a structure since stiffness and strength can be varied to

† Currently works at Nuclear Department of Babcock & Wilcox Canada, P.O. Box 310, Cambridge, Ontario, Canada N1R 5V3.

0022-460X/02/$35.00

suit the applied loads. The accurate prediction of the dynamic response (or failure characteristics) of structures made with advanced composite materials requires a refined shell theory, where the effect of transverse shear deformation and other factors (such as rotary inertia and initial curvature) are taken into account. Librescu [1] found, in the case of anisotropic plate, that the rotary inertia effect was practically inexistant at least at the lowest branch of the frequency spectrum. On the other hand, transverse shear deformation reduces the effective flexural stiffness of plates and shells in a different way for laminated composite materials from that for isotropic materials; the present study focuses on this last effect. This paper is based on the method developed by the authors [2], which deals with a generalization of geometrically linear first order shear deformation theory for multilayered anisotropic shells of general shape.

The fluid–shell interaction phenomenon is encountered when, for example, shells are partially filled with a stationary liquid, where the free surface motion of the fluid couples to the shell motion, and effects non-sloshing. This particular type of interaction occurs in the liquid-propellant tanks of rockets and in railroad cars used for the transportation of liquids. Another important source of fluid–shell interaction occurs when there is fluid flow with respect to the shell. Depending on the boundary conditions, static (buckling) and dynamic (flutter) instabilities are possible in the beam modes and also in the shell modes at sufficiently high flow velocities.

This paper is an attempt to determine the natural frequencies of anisotropic cylindrical shells, Figures 1 and 2, partially or completely filled with fluid or subjected to a flowing fluid. These frequencies are obtained for the following two cases of circumferential modes: axisymmetric ($n = 0$) and beam-like ($n = 1$). It should be noted that the lowest frequencies are not generally associated with these two modes. Deformations in these modes involve more strain energy than do deformations in modes where $n \geqslant 2$. In this investigation, the cylinder is vertical and free surface effects of the liquid, such as sloshing, are not taken into account.

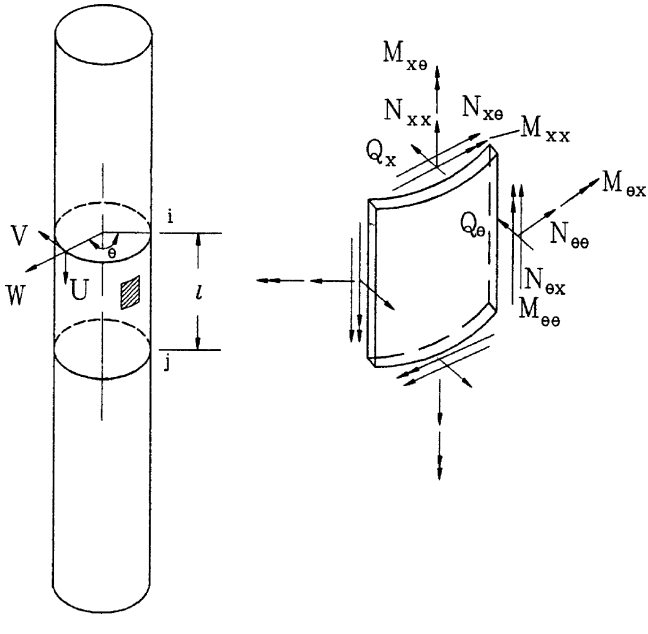

Figure 1. Cylindrical shell with differential element.

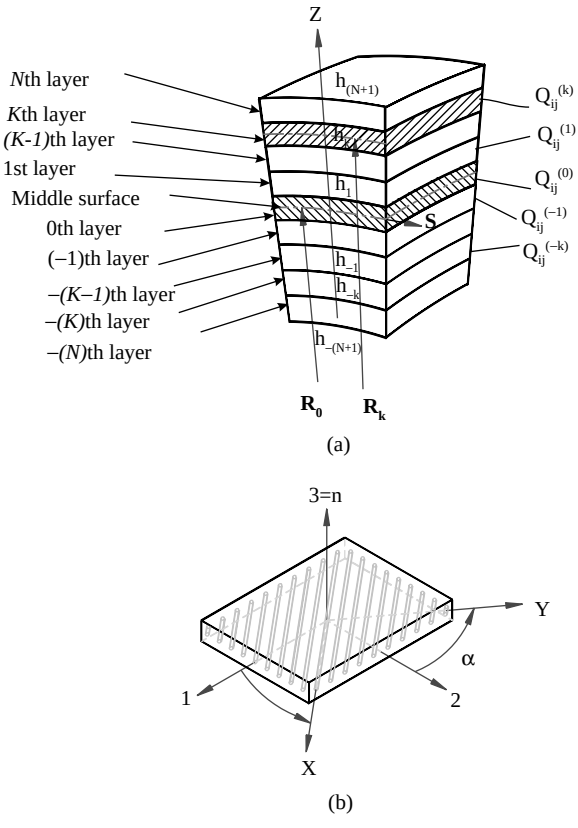

Figure 2. (a) Multidirectional laminate with co-ordinate notation of individual plies. (b) A fiber-reinforced lamina with global and material co-ordinate systems.

A number of theories for the study of fluid–structure interaction can be found in the literature. The first studies, and those which constitute the basic theories for the behavior of a liquid inside a cylindrical, spherical or other shell, dated from the 19th century and can be found in the work of Lamb [3]. After World War II, technological and scientific advances gave a new impetus to this field as programs were developed for research into space flight.

The free vibration of a fluid-filled circular cylindrical shell made of isotropic materials and filled with fluid has been well studied on the basis of classical shell theory. Excellent work on the subject is outlined in references [4–6]. Païdoussis [4] presents a dynamic study, both analytically and experimentally, of slender structures, mainly cylindrical bodies, in contact with axial flow, such that the structure either contains the flow or is submerrged in it, or both. Flow-induced instabilities, both static (divergence) and dynamic (flutter) instabilities, have been throughly studied in this monograph. The dynamic behavior of curved and straight pipes conveying fluid for both conservative systems and non-conservative ones is discussed, see reference [4], based on analytical approaches and the relevant experimental research.

Some analytical tools for the analysis of the vibrations of structures exposed to a fluid flow are given by Blevin [5], in which the vibrations of bluff structures induced by a subsonic flow are also studied. Different types of flow-induced vibrations are well classified

and described. The effects of oscillatory flow, turbulence and sound on the structure as well as flow-induced sound (aeroacoustic) are investigated, see reference [5].

Abramson [6] discusses the dynamic behavior of liquids in a moving container, such as the interaction between liquid propellants and the elastic structure of the container, the control and stability of moving liquids in the propellant tanks and the effects of lateral sloshing on a moving container. Some numerical methods such as the finite element approach and modal reduction procedures are presented by Morand and Ohayon [7] for the linear vibration analysis of elastic structures coupled to internal fluids.

Lakis and Païdoussis [8] developed a hybrid finite element, based on Sanders' theory [9], to investigate thin cylindrical shells partially filled with stationary liquid. Lakis and Sinno [10] applied the same method to the study of the free vibration characteristics of axisymmetric and beam-like cylindrical shells partially filled with liquid. Selmane and Lakis [11] also presented this method in their analysis of the free vibration of orthotropic open cylindrical shells subjected to a flowing fluid. For more details, the reader may be referred to Toorani and Lakis [2].

2. METHOD OF ANALYSIS

This work is based on the following assumptions: (1) the normal stress is assumed to be negligible compared to stress tangential to the shell surface; (2) general strain–displacement relations are expressed in arbitrary orthogonal curvilinear co-ordinates; (3) the linear elastic behavior of laminated anisotropic materials; (4) the effects of transverse shear deformation and rotary inertia forces are included in the shell model.

The method used is that developed by Toorani and Lakis [2, 12, 13], specifically for cylindrical shells with a circumferential mode equal to or greater than 2 ($\mathbf{n} \geqslant 2$). A cylinder, or any other shell undergoing free vibrations, may be deformed in a variety of ways, as shown in Figure 3, where several configurations are given. Viewed from one end, the vibration of the cylinder may consist of any number of waves distributed around the circumference. Denoting the number of these waves by n, we see, in Figure 3(a), cases of n equal to 0–4. When viewed from its side, the deformation of the cylinder consists of a number of waves distributed along the length of a generator. The appearance of the axial waveforms is, however, dependent upon the end conditions of the cylinder. For example, if the ends of cylinder are completely free, the motion of all points along the length of a given generator is the same. If the cylinder ends are simply supported, that is, maintained circular and free of axial moment, the axial waveforms are as shown in Figure 3(b). If we denote the number of axial half waves by m, then Figure 3(b) depicts cases in which m equals 1–3. On the other hand, if the ends of the cylindrical shell are clamped, the circumferential waveforms will again be as shown in Figure 3(a) while the axial waveforms will be distorted as shown in Figure 3(c) so as to conform. It is interesting, therefore, to realize, from a consideration of the axial waveforms, that for each type of end support the deformation of a generator of the shell resembles that of a beam which has the same end conditions as the shell. This fact will be shown to have analytical significance presently. As a pictorial summary of the vibration forms of a cylindrical shell, we have shown, in Figure 3(d), the nodal pattern of a shell with $n = 3$ and $m = 4$, wherein the nodal lines and circles are the loci of points whose radial deflection is constant. With this information at hand, we may now proceed to the analysis of a typical free vibration problem of the anisotropic circular cylindrical shell, Figures 1 and 2, in the cases of

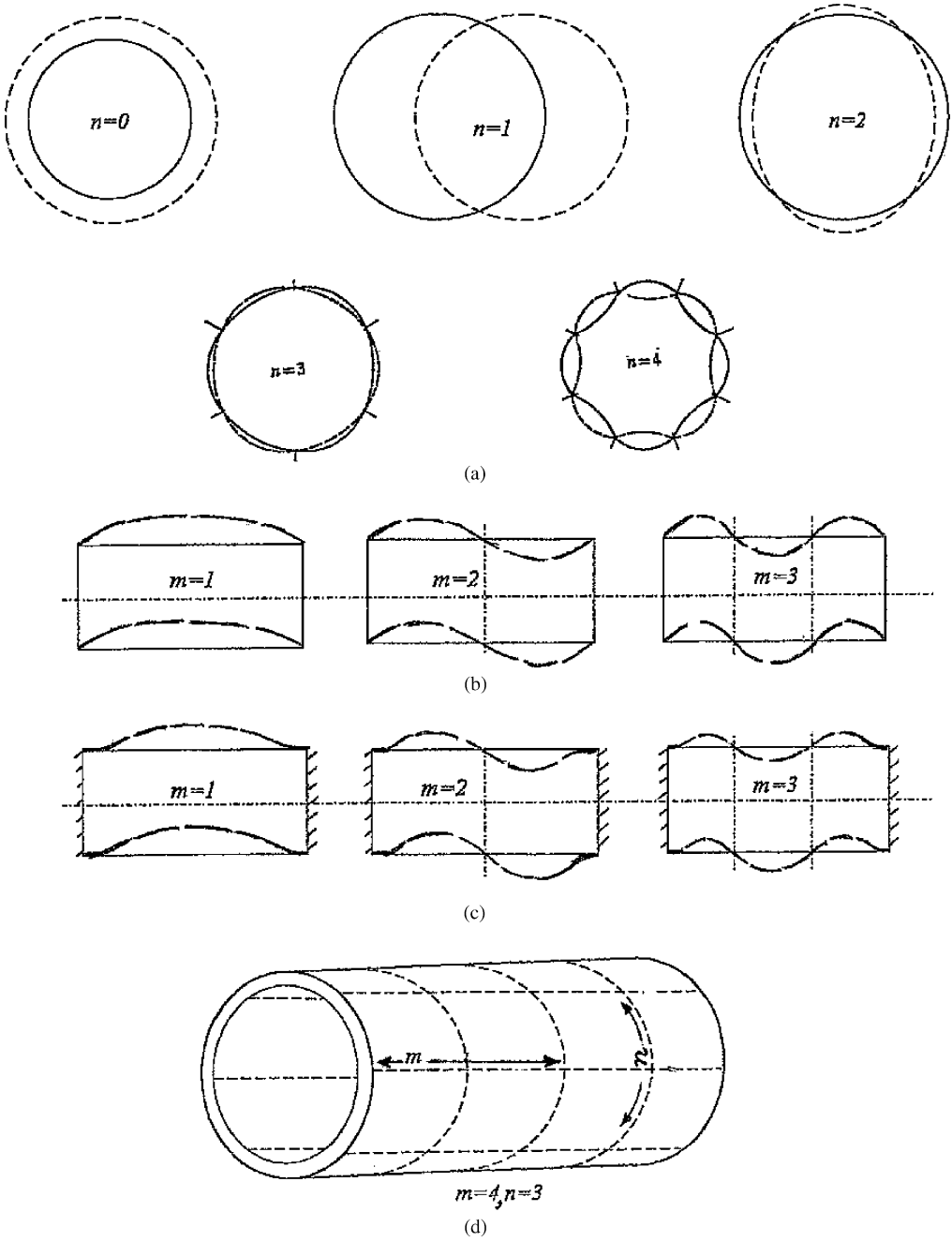

Figure 3. Vibration forms for circular cylindrical shells: (a) circumferential vibration forms ($n = 0-4$); (b) axial vibration forms in the case of simply supported ends; (c) axial waveforms of cylindrical shells in the case of the clamped ends; (d) nodal pattern of a cylindrical shell ($n = 3$ and $m = 4$).

axisymmetric ($n = 0$) and beam-like behavior ($n = 1$), Figure 3(a). The principal features of this method are as follows:

(1) The shell is subdivided into several cylindrical elements defined by two nodes "**i**" and "**j**" and the boundaries of the nodal surface (Figures 4 and 5). The displacement functions

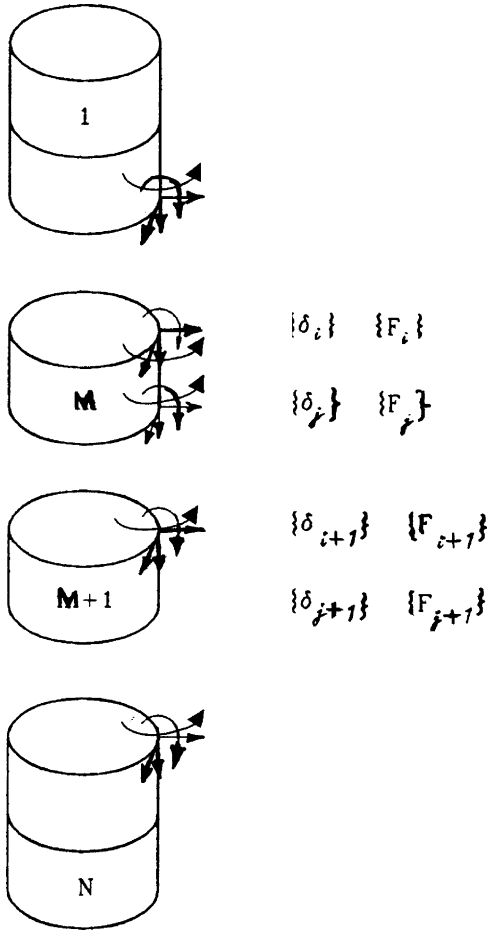

Figure 4. Division of the shell.

can be determined by

$$\begin{Bmatrix} U(x,\theta) \\ V(x,\theta) \\ W(x,\theta) \\ \beta_x(x,\theta) \\ \beta_\theta(x,\theta) \end{Bmatrix} = [N] \begin{Bmatrix} \delta_i \\ \delta_j \end{Bmatrix}, \tag{1}$$

where δ_i and δ_j represent the nodal displacements and $[N]$ is a matrix of shape functions.

(2) The displacement functions chosen must adequately represent the real displacement of the shell. As stated, in the present theory we employ the equations based on the shell theories (in which transverse shear deformation and rotary inertia effects are taken into account) to obtain the pertinent displacement function, instead of using the more common arbitrary polynomial forms. This is the point of departure of the present theory from what might be termed classical finite element theory. Five second order differential equations are obtained as a function of axial, radial and circumferential displacements of the mean

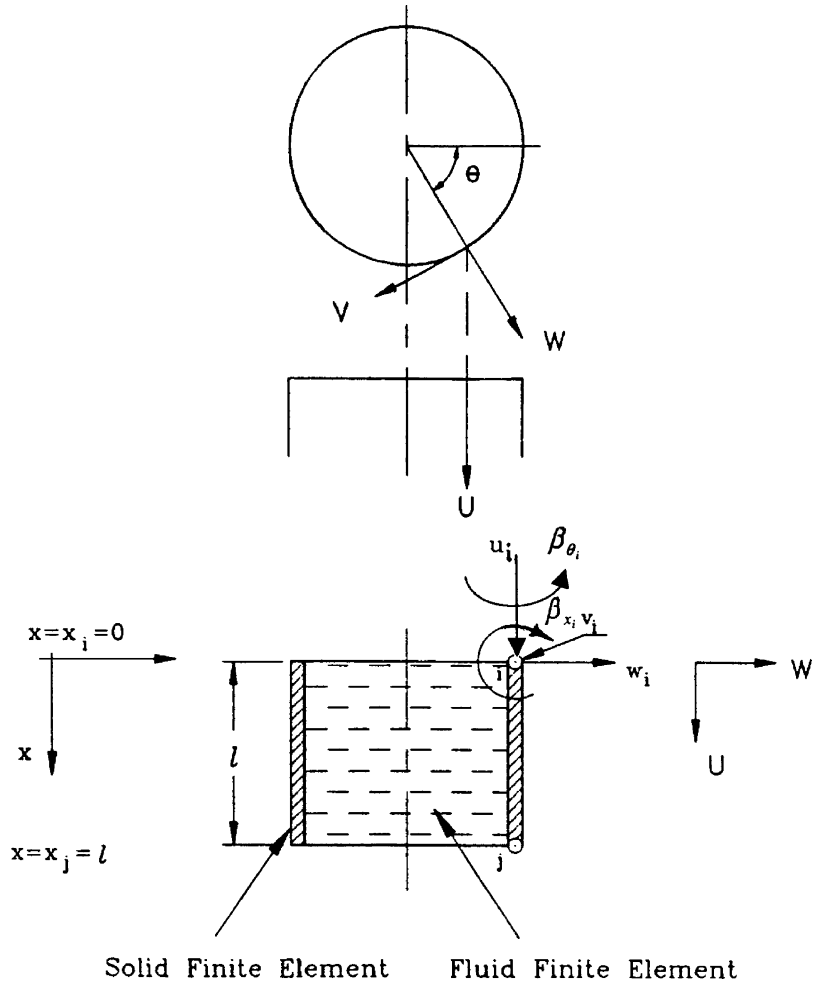

Figure 5. Displacements and degrees of freedom at a node.

surface of the shell as well as the rotations of the normal about the co-ordinates of the structure.

3. EQUATIONS OF MOTION

The principle of virtual work has been used in order to obtain the governing equilibrium equations based on assumed displacements. These equations have been developed by Toorani and Lakis [2]. These five equations of motion are implicit relations among 10 resultant forces and moments. There are five independent boundary conditions to be applied at given edges. The effect of transverse shear deformations is included in the present theory. The sixth equation of equilibrium is identically satisfied by the integral definitions of the shearing-stress resultants in terms of the shearing-stress components. For the classical theory of isotropic shells, such modified stress resultants and stress couples have been defined by Sanders [9]. For orthotropic and anisotropic shells, similar stress resultants and stress couples were considered by Librescu [1].

Based on Green's exact strain–displacement relations expressed in arbitrary orthogonal curvilinear co-ordinates, the strain–displacement relations for the shell are given by the following relation:

$$\{\varepsilon\} = \begin{Bmatrix} \varepsilon_x^0 \\ \gamma_x^0 \\ \mu_x^0 \\ \varepsilon_\theta^0 \\ \gamma_\theta^0 \\ \mu_\theta^0 \\ \kappa_x \\ \tau_x \\ \kappa_\theta \\ \tau_\theta \end{Bmatrix} = \begin{Bmatrix} \dfrac{\partial U}{\partial x} \\ \dfrac{\partial V}{\partial \theta} \\ \dfrac{\partial W}{\partial x} + \beta_x \\ \dfrac{1}{R}\dfrac{\partial V}{\partial \theta} + \dfrac{W}{R} \\ \dfrac{1}{R}\dfrac{\partial U}{\partial \theta} \\ \dfrac{1}{R}\dfrac{\partial W}{\partial \theta} - \dfrac{V}{R} + \beta_\theta \\ \dfrac{\partial \beta_x}{\partial x} \\ \dfrac{\partial \beta_\theta}{\partial x} + \dfrac{1}{2R}\dfrac{\partial V}{\partial x} \\ \dfrac{1}{R}\dfrac{\partial \beta_\theta}{\partial \theta} \\ \dfrac{1}{R}\dfrac{\partial \beta_x}{\partial \theta} - \dfrac{1}{2R^2}\dfrac{\partial U}{\partial \theta} \end{Bmatrix}_{(10\times 1)}, \tag{2}$$

where $\varepsilon_i^0, \gamma_i^0, \kappa_i, \tau_i$ and μ_i^0 are, respectively, the normal and in-plane shearing strain, the change in the curvature and torsion of the reference surface, and the shearing strain components. The constitutive relations for anisotropic laminated cylindrical shells, Figures 1 and 2, can be written as

$$\{N_{xx}, N_{x\theta}, Q_{xx}, N_{\theta\theta}, N_{\theta x}, Q_{\theta\theta}, M_{xx}, M_{x\theta}, M_{\theta\theta}, M_{\theta x}\}^{\mathrm{T}} = [P]_{(10\times 10)}\{\varepsilon\}, \tag{3}$$

where $\{\varepsilon\}$ and $[P]$ are, respectively, the deformation vector defined by equation (2) and the anisotropic matrix of elasticity, P_{ij}'s elements are given in reference [2].

In composite laminated plates and shells, the transverse shear stresses vary through the layer thickness. The discrepancy between the actual transverse shear stresses state and the constant ones through the thickness as occurring within the first order transverse shear deformation theory is often corrected in computing the transverse shear force resultants (Q_{xx} and $Q_{\theta\theta}$) using the shear correction factor. This factor is computed such that the strain energy due to transverse shear stresses equals the strain energy due to the true transverse stresses predicted by the three-dimensional elasticity theory. This factor depends, in general, on the lamination parameters such as number of layers, stacking sequence, degree of orthotropy and fiber orientation in each individual layer.

The equations of motion for cylindrical shells in terms of axial, tangential and radial displacements (u, v, w) of the mean surface of the shell, rotations of the normal about the axes of the shell (β_x and β_θ) and in terms of P_{ij}'s elements are given by

$$L_m\big(U, V, W, \beta_x, \beta_\theta, P_{ij}\big) = 0, \quad m = 1, \ldots, 5, \tag{4}$$

where $L_m (m = 1, 2, \ldots, 5)$ are five linear differential operators, the form of which is fully explained in reference [2]. The equations for the two cases studied here, $\mathbf{n} = 0$ and 1, are given in Appendix A. These governing equations have been developed in terms of

displacement measures. Therefore, the five necessary boundary conditions must be specified on each edge of the shell.

The free vibration of an anisotropic, laminated, composite, circular, cylindrical shell is studied using the hybrid finite element approach, in which a combination of the shear deformation theory of shells and the finite element method is used to derive the displacement functions. The symmetric and antisymmetric modes in the circumferential direction are coupled with each other due to the presence of in-plane extensional-shear, extensional-bending, bending–twisting, bending–shearing and twisting–stretching coupling in laminated composite shells.

4. DETERMINATION OF THE DISPLACEMENT FUNCTIONS

In accordance with the hybrid method proposed in section 2, the shell is subdivided into several uniform cylindrical elements, Figure 4. The cylindrical element is defined by two nodes $\mathbf{i}, \mathbf{j}$ and the three components U, V and W, respectively, represent the axial, tangential and radial displacements from a point located on the reference surface of the shell, and by two rotations.

4.1. CIRCUMFERENTIAL MODE $\mathbf{n} = 1$ (BEAM-LIKE)

The displacement functions can be written as

$$\begin{Bmatrix} U \\ V \\ W \\ \beta_x \\ \beta_\theta \end{Bmatrix} = [T]_{(5\times5)} \begin{Bmatrix} A\mathrm{e}^{\lambda x/R} \\ B\mathrm{e}^{\lambda x/R} \\ C\mathrm{e}^{\lambda x/R} \\ D\mathrm{e}^{\lambda x/R} \\ E\mathrm{e}^{\lambda x/R} \end{Bmatrix}, \tag{5}$$

where $[T]$ is given in Appendix B. Substituting equation (5) in equations of motion (4), for case $\mathbf{n} = 1$ given in Appendix A as equations (A.1)–(A.5), we obtain five homogeneous equations which are functions of constants A, B, C, D and E:

$$[H_1]\{ A \quad B \quad C \quad D \quad E \}^{\mathrm{T}} = 0. \tag{6}$$

In order to arrive at a non-trivial solution, the determinant of matrix $[H_1]$ must vanish. From this the following characteristic equation is derived.

$$|H_1| = f_{10}\lambda^{10} + f_8\lambda^8 + f_6\lambda^6 + f_4\lambda^4 + f_2\lambda^2 + f_0 = 0, \tag{7}$$

where f_i $(i = 0{-}10)$ are the coefficients of the determinant of five simultaneous algebraic equations; the elements of matrix $[H_1]$ are given in Appendix B. Each root λ_i, yields a solution to equation (4). The complete solution of the equations of motion is obtained by totaling the sum of the 10 independent solutions of equation (4), obtained for each constant λ_i $(i = 1, 2, \ldots, 10)$.

As A_i, B_i, C_i, D_i and E_i are not independent, we can write

$$A_i = \alpha_i C_i, \quad B_i = \beta_i C_i, \quad D_i = \gamma_i C_i, \quad \text{and} \quad E_i = \delta_i C_i \quad (i = 1, 2, \ldots, 10). \tag{8}$$

The displacements $U(x, \theta), V(x, \theta)$ and $W(x, \theta)$ as well as $\beta_x(x, \theta)$ and $\beta_\theta(x, \theta)$ can then be expressed in conjunction with the 10 C_i constants only, which can be determined

using 10 boundary conditions:

$$\begin{Bmatrix} U(x,\theta) \\ V(x,\theta) \\ W(x,\theta) \\ \beta_x(x,\theta) \\ \beta_\theta(x,\theta) \end{Bmatrix} = [T]_{(5\times5)}[R_1]_{(5\times10)}\{C\}_{(10\times1)}, \tag{9}$$

where $[R_1]$ is given in Appendix B and $\{C\}$ is a vector of constants which are linear combinations of the C_i. The nodal displacement vector is now expressed as

$$\{\delta_i\} = \begin{Bmatrix} u_i & v_i & w_i & \beta_{x_i} & \beta_{\theta_i} \end{Bmatrix}^{\mathrm{T}}. \tag{10}$$

Each element has two nodes and 10 degrees of freedom and x has a definite value ($x = 0$ at node **i**) and ($x = \ell$ at node **j**), so the element displacements at the boundaries can be given by the relation

$$\begin{Bmatrix} \delta_{1i} \\ \delta_{1j} \end{Bmatrix} = \begin{Bmatrix} u_i & v_i & w_i & \beta_{x_i} & \beta_{\theta_i} & u_j & v_j & w_j & \beta_{x_j} & \beta_{\theta_j} \end{Bmatrix}^{\mathrm{T}} = [A_1]_{(10\times10)}\{C\}_{(10\times1)}, \tag{11}$$

where the elements of matrix $[A_1]$ are obtained from those of matrix $[R_1]$ and given in Appendix B. Substituting this definition into equation (9), we get

$$\begin{Bmatrix} U(x,\theta) \\ V(x,\theta) \\ W(x,\theta) \\ \beta_x(x,\theta) \\ \beta_\theta(x,\theta) \end{Bmatrix} = [T][R_1][A_1]^{-1}\begin{Bmatrix} \delta_{1i} \\ \delta_{1j} \end{Bmatrix} = [N_1]\begin{Bmatrix} \delta_{1i} \\ \delta_{1j} \end{Bmatrix}. \tag{12}$$

These equations determine the displacement functions. $[T]$ is given in equation (5), the matrices $[R_1]$ and $[A_1]$ are listed in Appendix B, and $\{\delta_{1i}\}$ and $\{\delta_{1j}\}$ are the displacements at the boundaries "*i*" and "*j*" of one element, see Figure 5.

4.2. CIRCUMFERENTIAL MODE $\mathbf{n} = 0$ (AXISYMMETRIC CASE)

In the particular case of axisymmetric motion, the displacements are a function of x only, and the motions of equations are given in Appendix A as equations (A.6)–(A.10). Two systems of equations have been obtained: one, the so-called torsional system is represented by equations for L_2^0 and L_5^0, given in Appendix A, and is a function of V and β_θ only; the other is a non-torsional system, represented by equations for L_1^0, L_3^0 and L_4^0 given in Appendix A, which is a function of U, W and β_x.

4.2.1. *Non-torsional system*

Assuming

$$U(x) = Ae^{\lambda x/R}, \quad W(x) = Ce^{\lambda x/R}, \quad \beta_x(x) = De^{\lambda x/R} \tag{13}$$

and substituting equation (13) into the three equations of motion related to this case, we obtain three homogeneous equations which are functions of constants A, C and D:

$$[H_0]\begin{Bmatrix} A & C & D \end{Bmatrix}^{\mathrm{T}} = 0. \tag{14}$$

Considering the non-trivial solution of equation (14), the following characteristic equation is obtained for the non-torsional case of axisymmetric mode:

$$|H_0| = f_6^0 \lambda^6 + f_4^0 \lambda^4 + f_2^0 \lambda^2 = 0. \tag{15}$$

Matrix $[H_0]$ and the values of coefficient f_i^0 in this polynomial equation are given in Appendix C. Assuming $A_j = \alpha_j C_j$, $D_j = \gamma_j C_j$ and substituting them in equation (13), we obtain

$$\begin{Bmatrix} U \\ W \\ \beta_x \end{Bmatrix} = [R_0]_{(3\times6)}\{C\}_{(6\times1)}, \tag{16}$$

where $[R_0]$ is given in Appendix C. To determine the six C_j constants, six boundary conditions for each element must be formulated. To this end, displacements for boundaries $i(x = 0)$ and $j(x = \ell)$ are expressed by

$$\begin{Bmatrix} \delta_{0i} \\ \delta_{0j} \end{Bmatrix} = \{ u_i \quad w_i \quad \beta_{xi} \quad u_j \quad w_j \quad \beta_{xj} \}^{\mathrm{T}} = [A_0]_{(6\times6)}\{C\}_{(6\times1)}. \tag{17}$$

The matrix $[A_0]$ is given in Appendix C and vector $\{C\}$ is given by

$$\{C\} = [A_0^{-1}] = \begin{Bmatrix} \delta_i^0 \\ \delta_j^0 \end{Bmatrix}. \tag{18}$$

Substituting equation (18) into equation (16), we obtain

$$\begin{Bmatrix} U(x) \\ W(x) \\ \beta_x(x) \end{Bmatrix} = [R_0][A_0^{-1}]\begin{Bmatrix} \delta_i^0 \\ \delta_j^0 \end{Bmatrix} = [N_0]\begin{Bmatrix} \delta_i^0 \\ \delta_j^0 \end{Bmatrix}. \tag{19}$$

4.2.2. *Torsional system*

The displacement functions can be represented by

$$V(x) = B_0 + B_1 x \quad \text{and} \quad \beta_\theta(x) = E_0 + E_1 x \tag{20}$$

such that

$$\begin{Bmatrix} V(x) \\ \beta_\theta(x) \end{Bmatrix} = [R_0'][A_0']^{-1}\begin{Bmatrix} \delta_{0i}' \\ \delta_{0j}' \end{Bmatrix}, \tag{21}$$

where

$$\begin{Bmatrix} \delta_{0i}' \\ \delta_{0j}' \end{Bmatrix} = \begin{Bmatrix} v_i \\ \beta_{\theta i} \\ v_j \\ \beta_{\theta j} \end{Bmatrix} = [A_0']_{(4\times4)}\begin{Bmatrix} B_0 \\ E_0 \\ B_1 \\ E_1 \end{Bmatrix} \tag{22}$$

and matrices $[A_0']$ and $[R_0']$ are given in Appendix C.

5. DETERMINATION OF MASS AND STIFFNESS MATRICES FOR THE STRUCTURAL ELEMENT

This section will cover determination of the mass and stiffness matrices and the method of constructing global matrices.

5.1. ARBITRARY LOAD IN BEAM-LIKE CONDITIONS ($\mathbf{n} = 1$)

5.1.1. *Strain–displacement relationships*

The strain vector $\{\varepsilon_1\}$ can now be expressed in terms of δ_i^1 and δ_j^1 using equations (2) and (12):

$$\{\varepsilon_1\}_{(10\times1)} = \begin{bmatrix} [T] & \\ & [T] \end{bmatrix}_{(10\times10)} [Q_1]_{(10\times10)} \left[A_1^{-1}\right]_{(10\times10)} \begin{Bmatrix} \delta_{1i} \\ \delta_{1j} \end{Bmatrix}_{(10\times1)}, \tag{23}$$

where matrices $[A_1]$ and $[Q_1]$ are given in Appendix B and $\{\varepsilon_1\}$ is given by equation (2).

5.1.2. *Stress–strain relationships*

Using equations (3) and (23), the corresponding stress–strain relationships can be written as

$$\{\sigma_1\} = [P_1]_{(10\times10)} [B_1]_{(10\times10)} \begin{Bmatrix} \delta_i^1 \\ \delta_j^1 \end{Bmatrix}_{(10\times1)}. \tag{24}$$

The P_{ij}'s elements describe the shell anisotropy which depends on the mechanical properties of the material of the structure. Some coupling, such as in-plane extensional shear, extensional bending and bending–twisting, can be present in anisotropic laminated composite shells due to the asymmetry of the scheme lamination or fiber orientation. Some of the P_{ij}'s elements can, therefore, be null or not *null*. The mass and stiffness matrices for one finite element can be expressed as

$$[m_s] = \rho_s t \iint [N]^{\mathrm{T}} [N] \, \mathrm{d}A, \quad [k_s] = \iint [B]^{\mathrm{T}} [P] [B] \, \mathrm{d}A, \tag{25}$$

where $\mathrm{d}A = r \, \mathrm{d}x \, \mathrm{d}\theta$ and matrices $[P]$, $[N]$ and $[B]$ are defined in equations (3), (12) and (24); substituting them in equation (25) and doing the analytical integration with respect to x and θ, we obtain

$$[m_{1s}]_{(10\times10)} = \rho_s t \left[A_1^{-1}\right]^{\mathrm{T}} [S_1] \left[A_1^{-1}\right], \quad [k_{1s}]_{(10\times10)} = \left[A_1^{-1}\right]^{\mathrm{T}} [G_1] \left[A_1^{-1}\right]. \tag{26}$$

The elements of matrices $[S_1]$ and $[G_1]$ are determined in conjunction with elements of matrix $[P]$, $\lambda, \alpha, \beta, \delta$ and γ:

$$\begin{aligned} S_1(i,j) &= \pi R^2 \Gamma_1(i,j) \frac{1}{(\lambda_i + \lambda_j)} \left[\mathrm{e}^{(\lambda_i+\lambda_j)\ell/R} - 1 \right], \\ G_1(i,j) &= \pi R^2 \Pi_1(i,j) \frac{1}{(\lambda_i + \lambda_j)} \left[\mathrm{e}^{(\lambda_i+\lambda_j)\ell/R} - 1 \right], \end{aligned} \quad \text{if } \lambda_i + \lambda_j \neq 0. \tag{27}$$

and

$$\begin{aligned} S_1(i,j) &= \pi R \ell \Gamma_1(i,j) \\ G_1(i,j) &= \pi R \ell \Pi_1(i,j) \end{aligned} \quad \text{if } \lambda_i + \lambda_j = 0, \tag{28}$$

where $\Gamma_1(i,j)$ and $\Pi_1(i,j)$ are given in Appendix B.

5.2. SYMMETRIC LOAD ($\mathbf{n} = 0$)

Situation here is as in the case involving arbitrary loads.

5.2.1. *Non-torsional case*

The strain vector for this case can be defined as

$$\{\varepsilon_0\}_{(4\times1)} = [Q_0]_{(4\times6)}\left[A_0^{-1}\right]_{(6\times6)}\begin{Bmatrix}\delta_{0i}\\ \delta_{0j}\end{Bmatrix}, \tag{29}$$

where the vector $\{\varepsilon_0\}$ and matrices $[Q_0]$ and $[A_0]$ are given in Appendix C. The mass and stiffness matrices are obtained as

$$[m_{0s}]_{(6\times6)} = \rho_s t\left[A_0^{-1}\right]^{\mathrm{T}}[S_0]\left[A_0^{-1}\right], \quad [k_{0s}]_{(6\times6)} = \left[A_0^{-1}\right]^{\mathrm{T}}[G_0]\left[A_0^{-1}\right], \tag{30}$$

where

$$\begin{aligned} G_0(i,j) &= \frac{2\pi R^2}{(\lambda_i+\lambda_j)}\Pi_0(i,j)\left(\mathrm{e}^{(\lambda_i+\lambda_j)\ell/R}-1\right), \\ S_0(i,j) &= \frac{1}{2}G_0(i,j)\frac{\Gamma_0(i,j)}{\Pi_0(i,j)}, \end{aligned} \quad \text{if } (\lambda_i+\lambda_j)\neq 0.$$

$$\begin{aligned} G_0(i,j) &= 2\pi R\ell\Pi_0(i,j), \\ S_0(i,j) &= 2\pi R\ell\Gamma_0(i,j), \end{aligned} \quad \text{if } (\lambda_i+\lambda_j)=0, \tag{31}$$

where $\Pi_0(i,j)$ and $\Gamma_0(i,j)$ are given in Appendix C.

5.2.2. *Torsional case*

The strain–displacement relationship for this case is obtained as

$$\left\{\varepsilon_0'\right\} = \left[Q_0'\right]_{(3\times4)}\left[A_0'\right]_{(4\times4)}\begin{Bmatrix}\delta_{0i}'\\ \delta_{0j}'\end{Bmatrix}, \tag{32}$$

where the vector $\{\varepsilon_0'\}$ and matrices $[Q_0']$ and $[A_0']$ are given in Appendix C and

$$\begin{Bmatrix}\delta_{0i}'\\ \delta_{0j}'\end{Bmatrix} = \begin{Bmatrix} v_i & \beta_{\theta i} & v_j & \beta_{\theta j}\end{Bmatrix}^{\mathrm{T}}. \tag{33}$$

The mass and stiffness matrices for this case are defined as

$$\begin{aligned} &m_{0s}'(1,1) = m_{0s}'(2,2) = 3m_{0s}'(3,3) = 3m_{0s}'(4,4) = 2\pi R\ell\rho_s t, \\ &m_{0s}'(1,3) = m_{0s}'(3,1) = m_{0s}'(2,4) = m_{0s}'(4,2) = \pi R\ell\rho_s t, \\ &\text{other terms} = 0, \end{aligned} \tag{34}$$

and

$$R^2 k'_{0s}(1,1) = k'_{0s}(2,2) = aP_{66}, k'_{0s}(3,3) = a\left[\left(P_{22} + \frac{P_{28}}{R} + \frac{P_{88}}{4R^2}\right) + P_{66}\frac{\ell^2}{3R^2}\right],$$

$$k'_{0s}(4,4) = a\left(P_{88} + \frac{P_{66}\ell^2}{3}\right), k'_{0s}(1,2) = k'_{0s}(2,1) = -\frac{2R}{\ell}k'_{0s}(1,3) = -\frac{2R}{\ell}k'_{0s}(3,1) = -\frac{aP_{66}}{R},$$

$$k'_{0s}(2,3) = k'_{0s}(3,2) = \frac{-1}{R}k'_{0s}(2,4) = \frac{-1}{R}k'_{0s}(4,2) = \frac{-a\ell}{2R}P_{66}, k'_{0s}(1,4) = k'_{0s}(4,1) = -\frac{a\ell P_{66}}{2R},$$

$$k'_{0s}(3,4) = k'_{0s}(4,3) = a\left[\left(P_{28} + \frac{P_{88}}{2R}\right) - \frac{\ell^2}{3R}P_{66}\right],$$

where

$$a = \pi R\ell. \tag{35}$$

6. DYNAMICS BEHAVIOR OF FLUID–STRUCTURE INTERACTION

This section covers the final formulations of the equations of motion for cylindrical shells completely or partially filled with liquid or subjected to a flowing fluid, by using the relationships established in this paper.

6.1. EQUATIONS OF MOTION

The equations of motion of a shell interacting with a fluid can be represented as

$$\left([M_s] - [M_f]\right)\{\ddot{\delta}\} - [C_f]\{\dot{\delta}\} + \left([K_s] - [K_f]\right)\{\delta\} = \{F\}, \tag{36}$$

where subscripts '*s*' and '*f*' refer to the shell *in vacuo* and fluid filled respectively. $[M_s]$ and $[K_s]$ are, respectively, the global mass and stiffness matrices of the shell *in vacuo*. The $[M_f]$, $[C_f]$ and $[K_f]$ represent the inertial, Coriolis and centrifugal forces of the fluid flow, $\{\delta\}$ is the displacement vector and $\{F\}$ represents the external forces.

6.2. INERTIAL, CORIOLIS AND CENTRIFUGAL FORCES OF THE FLOW

We assume that the shell is subjected only to a potential flow which induces inertial, Coriolis and centrifugal forces to participate in the vibration pattern. These forces are coupled with the elastic deformation of the shell. The mathematical model developed here is based on the following assumptions: (1) The fluid flow is potential; (2) the fluid is assumed to be inviscid, incompressible and irrotational; (3) the deformations are small, allowing the use of linear theory; (4) the fluid mean velocity distribution is assumed to be constant across a shell section.

6.3. DETERMINATION OF THE APPARENT MASS, STIFFNESS AND DAMPING MATRICES OF THE FLUID FLOW

The velocity function Φ, considering the assumptions of section 6.2, in the cylindrical co-ordinate system is expressed by

$$\frac{\partial^2\Phi}{\partial r^2} + \frac{1}{r}\frac{\partial\Phi}{\partial r} + \frac{1}{r^2}\frac{\partial^2\Phi}{\partial\theta^2} + \frac{\partial^2\Phi}{\partial x^2} = 0, \tag{37}$$

where 'Φ' is the potential function. The components of the flow velocity are given by

$$V_x = U_x + \frac{\partial \Phi}{\partial x}, \quad V_\theta = \frac{1}{R}\frac{\partial \Phi}{\partial \theta}, \quad V_r = \frac{\partial \Phi}{\partial r}, \tag{38}$$

where U_x is the velocity of the fluid through the shell section, V_x, V_θ and V_r are, respectively, the axial, tangential and radial components of the fluid velocity. Using Bernoulli's equation for steady flow,

$$\left(\frac{\partial \Phi}{\partial t} + \frac{V^2}{2} + \frac{P}{\rho_f}\right)\bigg|_{r=\xi} = 0. \tag{39}$$

Substituting for V^2, the dynamic pressure 'P' can be found as

$$P_{i,e} = -\rho_{f_{i,e}}\left(\frac{\partial \Phi_{i,e}}{\partial t} + U_{xi,e}\frac{\partial \Phi_{i,e}}{\partial x} + \frac{U_{xi,e}^2}{2} + \frac{1}{2}\left[\left(\frac{\partial \Phi_{i,e}}{\partial x}\right)^2 + \frac{1}{r^2}\left(\frac{\partial \Phi_{i,e}}{\partial \theta}\right)^2 + \left(\frac{\partial \Phi_{i,e}}{\partial r}\right)\right]\right)_{r=R_{i,e}=R\mp t/2} \tag{40}$$

in which the subscript i and e represent *internal* or *external* locations of the structure. A full definition of the flow requires that a condition be applied to the shell–fluid interface. The impermeability condition of the shell surface requires that the radial velocity of the fluid, on the shell surface, should match the instantaneous rate of change of the shell displacement in the radial direction. This condition implies a permanent contact between the shell surface and the peripheral fluid layer, which should be

$$V_r|_{r=R} = \frac{\partial \Phi}{\partial r}\bigg|_{r=R} = \left(\frac{\partial W}{\partial t} + U_x\frac{\partial W}{\partial x}\right)_{r=R}. \tag{41}$$

The differential equation can be solved using the separation of variables method. The radial displacement, from shell theory, is defined as

$$W(x,\theta,t) = \sum_{j=1}^{10} C_j \exp\left[\frac{\lambda_j x}{R} + \mathrm{i}\omega t\right]\cos\theta, \tag{42}$$

where λ_j is the jth root of the characteristic equation and ω is the natural angular frequency. The velocity potential is assumed to be

$$\Phi(x,\theta,r,t) = \sum_{j=1}^{10} R_j(r)S_j(x,\theta,t). \tag{43}$$

The function $S_j(x,\theta,t)$ can be explicitly determined after applying the impermeability condition (41) and using the radial displacement relation given by equation (42). Substituting the explicit term of $S_j(x,\theta,t)$ into equation (43), we obtain

$$\Phi(x,\theta,r,t) = \sum_{j=1}^{10} \frac{R_j(r)}{(\partial R_j(R)/\partial r)}\left[\frac{\partial W_j}{\partial t} + U_x\frac{\partial W_j}{\partial x}\right]. \tag{44}$$

Introducing this explicit term (44) and equation (42) into equation (37), we obtain Bessel's homogeneous differential equation:

$$r^2\frac{\mathrm{d}^2 R_j(r)}{\mathrm{d}r^2} + r\frac{\mathrm{d}R_j(r)}{\mathrm{d}r} + R_j(r)\left[\mathrm{i}^2 m_j^2 r^2 - n^2\right] = 0, \tag{45}$$

where 'i' is the complex number, $\mathrm{i}^2 = -1$ and m_j is defined as

$$m_j^2 = \left(\frac{\lambda_j}{R}\right)^2 - \frac{1}{C_f^2}\left(\omega + U_x\frac{\lambda_j}{R}\right)^2, \tag{46}$$

where λ_j, R, ω and U_x are the roots of the characteristic equation, the radius of the shell, the natural angular frequency and the flow velocity respectively. For shells in a liquid medium, $i^2 m_j^2$ is usually negative, and the general solution of equation (45) is given by

$$R_j(r) = A\mathrm{J}_{n_j}(\mathrm{i}m_j r) + B\mathrm{Y}_{n_j}(\mathrm{i}m_j r), \tag{47}$$

where J_{nj} and Y_{nj} are Bessel functions of the first and second kind and of order **n** respectively. For a shell filled with a liquid (internal flow), the constant 'B' has to be set equal to zero since the Y_{nj} is singular at $\mathbf{r} = 0$. For a shell submerged in a liquid (external flow), the constant 'A' is equal to zero. It is noted that for a shell in a fluid medium, the effect of the liquid is taken into account by considering an added mass. The complete solution is found when the shell is simultaneously subjected to internal and external flow.

An expression for dynamic pressure as a function of the displacement W_j and the function $R_j(r)$, taking into account only the linear terms, is obtained by substituting equation (44) and the first derivation of the Bessel function, of the first and second kind, into equation (40):

$$\begin{aligned} P = \sum_{q=1}^{10} \Bigg\{ & [\rho_e R_e Z_q^Y(m_q R) - \rho_i R_i Z_q^J(m_q R)] \frac{\partial^2 W_q}{\partial t^2} \\ & + 2[\rho_e R_e U_{x_e} Z_q^Y(m_q R) - \rho_i R_i U_{x_i} Z_q^J(m_q R)] \frac{\partial^2 W_q}{\partial t \partial x} \\ & + \left[\rho_e R_e U_{x_e}^2 Z_q^Y(m_q R) - \rho_i R_i U_{x_i}^2 Z_q^J(m_q R)\right] \frac{\partial^2 W_q}{\partial x^2} \Bigg\}, \end{aligned} \tag{48}$$

where $\rho_{e,i}$ is the density of external or internal fluid and

$$\begin{aligned} Z_q^J(m_q R) &= 1/[n - m_q R_i(\mathrm{J}_{n+1}(m_q R_i)/\mathrm{J}_n(m_q R_i)], \\ Z_q^Y(m_q R) &= 1/[n - m_q R_e(\mathrm{Y}_{n+1}(m_q R_e)/\mathrm{Y}_n(m_q R_e)]. \end{aligned} \tag{49}$$

When we substitute the nodal interpolation functions of the empty shell (12), which can be used for the fluid column, into the dynamic pressure expression (48) and carry out the necessary matrix operations by our chosen method, the mass, damping and stiffness matrices for the fluid are obtained by integrating the following integral with respect to x and θ:

$$\int_A [N]^{\mathrm{T}} \{P\} \, \mathrm{d}A. \tag{50}$$

Finally, the inertial, Coriolis and centrifugal forces due to a flowing fluid, neglecting the viscous term, are obtained by analytical integration of equation (50) and can be written as

$$[m_f] = \left[A_f^{-1}\right]^{\mathrm{T}} [S_f] \left[A_f^{-1}\right], \quad [c_f] = \left[A_f^{-1}\right]^{\mathrm{T}} [D_f] \left[A_f^{-1}\right], \quad [k_f] = \left[A_f^{-1}\right]^{\mathrm{T}} [G_f] \left[A_f^{-1}\right]. \tag{51}$$

The matrix $[A]$ is defined by equation (11) and the elements of $[S_f], [D_f]$ and $[G_f]$ matrices are given by

$$\begin{aligned} S_f(k,q) &= -\pi \Xi_{kq} (\rho_{fi} R_i^2 Z_{kq}^J - \rho_{fe} R_e^2 Z_{kq}^Y), \\ D_f(k,q) &= -2\lambda_q \pi \Xi_{kq} (\rho_{fi} R_i U_{x_i} Z_{kq}^J - \rho_{fe} R_e U_{x_e} Z_{kq}^Y), \\ G_f(k,q) &= -\pi \lambda_q^2 \Xi_{kq} (\rho_{fi} U_{x_i}^2 Z_{kq}^J - \rho_{fe} U_{x_e}^2 Z_{kq}^Y), \end{aligned} \tag{52}$$

where $i, j = 1, ..., 10$, ρ_f is the density of the fluid and subscripts i and e mean, respectively, internal and external flow. U_x is the velocity of the fluid, $Z_{kq}^{J,Y}$ is given in equations (49) and Ξ_{kq} is given in Appendix D.

The Coriolis force, $[c_f]$, results from the coupling of the relative velocity of the fluid with the rotation of a section of the structure. It is important to note that the centrifugal and Coriolis terms have a special importance here since they are responsible for the non-conservative aspects of the problems to be solved. Mathematically, they cause the differential equations that generate complex eigenvalue problems. Physically, the system experiences static (buckling) and dynamic (flutter) instability.

As long as the effective stiffness of the system remains positive as flow velocity increases, the system will oscillate asymptotically about its neutral equilibrium position; otherwise, it will diverge to a new equilibrium position, different from neutral (buckling). As long as the effective fluid damping of the system remains positive as flow velocity is increased, vibrations will be damped; otherwise, they will be amplified (flutter).

Note: The foregoing developments given for the fluid are valid for $n = 1$ and $n = 0$ as shown in the appropriate matrices, $[A_1]$ for $n = 1$ and $[A_0]$ for $n = 0$.

7. ANALYSIS OF FREE VIBRATION

The global matrices of each structure and fluid column are obtained by superimposing the mass and stiffness matrices for each individual element. After applying the boundary conditions, these matrices are reduced to square matrices of order $NDF(N+1) - NC$ where NDF, N and NC are, respectively, the number of degrees of freedom at each node, the number of elements and the restriction imposed. The equations of motion of a shell interacting with a fluid are

$$\left([M_s] - [M_f]\right)\{\ddot{\delta}\} - [C_f]\{\dot{\delta}\} + \left([K_s] - [K_f]\right)\{\delta\} = \{0\}, \tag{53}$$

where $[M_s]$ and $[K_s]$ are, respectively, the global mass and stiffness matrices for the empty shell, $[M_f]$ and $[K_f]$ are the global mass and stiffness matrices for the fluid and $[C_f]$ is the Coriolis force of the fluid. Equation (53) is thus solved to obtain $5(N+1) - NC$ eigenvalues and eigenvectors.

7.1. EIGENVALUE AND EIGENVECTOR PROBLEM

The eigenvalue and eigenvector problem is solved by means of the equation reduction technique. Equation (53) may be rewritten as

$$\begin{bmatrix} [0] & \frac{1}{\omega_0}[M] \\ \frac{1}{\omega_0^2}[M] & \frac{1}{\omega_0}[C] \end{bmatrix} \begin{Bmatrix} \ddot{\delta} \\ \dot{\delta} \end{Bmatrix} + \begin{bmatrix} -\frac{1}{\omega_0}[M] & [0] \\ [0] & [K] \end{bmatrix} \begin{Bmatrix} \dot{\delta} \\ \delta \end{Bmatrix} = \begin{Bmatrix} 0 \\ 0 \end{Bmatrix}, \tag{54}$$

where

$$[M] = [M_s] - [M_f], [K] = [K_s] - [K_f], [C] = [C_f], \tag{55}$$

and where $\omega_0 = p_{11}$ is the first element of the elasticity matrix. The eigenvalue problem is given by

$$|[DD] - \Lambda[I]| = 0, \tag{56}$$

where

$$[DD] = \begin{bmatrix} [0] & [I] \\ -\dfrac{1}{\omega_0^2}[K]^{-1}[M] & -\dfrac{1}{\omega_0^2}[K]^{-1}[C] \end{bmatrix} \tag{57}$$

and $\Lambda = 1/(\omega_0^2\omega^2)$; ω is the natural frequency of the system expressed in radians per second.

7.2. PARTICULAR CASE

The matrices $[K_f]$ and $[C_f]$ are not involved in computations in the case of non-flowing fluid ($U_{xi} = 0{\cdot}0$). The eigenvalue problem in this particular case may be reduced to

$$\left|\frac{1}{\omega_0^2}[K]^{-1}[M] - \Lambda[I]\right| = 0. \tag{58}$$

Matrices $[K]$, $[M]$ and $[C]$ are square matrices of order $NDF(N+1) - NC$, where NDF is the number of degrees of freedom at each node, N is the number of finite elements in the structure and NC is the number of constraints applied.

8. CALCULATIONS AND DISCUSSION

In this section, we apply the proposed method to the case of laminated anisotropic and isotropic cylindrical shells, partially or completely filled with fluid. The free surface effect is not taken into account. No dynamic pressure is imposed on the liquid free surface and the superficial tension is neglected. We justify this on the grounds that the natural frequencies of the empty shells in the modes under consideration are likely to be high, whereas the natural frequencies of the free surface phenomena are likely to be low, at least in the lowest modes. Accordingly, coupling between the shell modes and the liquid free surface modes may be expected to be weak.

The parametric values such as $R/t, L/R$, fluid depth ratio, as well as the circumferential and axial wave numbers, for all examples, are provided in the figures and tables. The values of the shear correction factors used in calculations have been taken as $\pi^2/12$. It should be noted that the results using Sanders' theory were obtained, in the present work, only when the transverse shear deformation effects were neglected.

8.1. NATURAL VIBRATION OF THE EMPTY CYLINDRICAL SHELL

Tables 1 and 2 show the non-dimensional natural frequencies computed for an empty simply supported cylindrical shell, for the beam-like ($n = 1$) mode and different values of the axial mode, along with the corresponding values obtained from other theories. The material properties for the isotropic case are $E = 203{\cdot}4\,\text{GPa}, \rho_s = 7812\,\text{kg/m}^3$, $v = 0{\cdot}3$ and $\rho_f = 1000\,\text{kg/m}^3$.

As can be seen, the difference between the results obtained from the present theory and those of classical shell theories increases as the axial mode (m) is increased and the L/R and R/t ratios are decreased.

Vibration parameters (Ω) of an empty cylindrical shell for axisymmetric case ($n=0$) are given in Table 3. It is observed that the R/t ratio has only a slight effect upon the results

TABLE 1

Frequency parameter ($\Omega = \omega r\sqrt{\rho(1-\nu^2)/E}$) of a simply supported cylindrical shell (empty, n=1)

L/R	$[R/t]$								
	10			20			100		
	m			m			m		
	1	3	5	1	3	5	1	3	5
0·5	1·1523	5·0401	10·372	1·0690	4·5719	8·797	1·0683	1·6439	3·2869
	1·5096	12·207	24·413	1·1291	6·1939	17·958	1·0816	1·7037	3·7633
1	0·81298	1·9024	3·9661	0·8560	1·4861	2·9439	0·8450	1·1465	1·4105
	0·90063	2·8661	8·1915	0·8581	1·6862	4·2191	0·8501	1·1526	1·4330
2	0·51360	0·99188	1·5679	0·5416	0·95831	1·2426	0·5601	1·0265	1·1058
	0·57744	1·1325	2·0846	0·5746	0·99041	1·3530	0·5849	1·0435	1·1154
5	0·18562	0·67281	0·84792	0·1826	0·66597	0·85979	0·1872	0·68610	0·93985
	0·18656	0·72448	0·90063	0·1870	0·67236	0·87556	0·1877	0·72187	0·96614
10	0·05510	0·32696	0·56990	0·0572	0·32730	0·5757	0·0582	0·33004	0·57278
	0·05920	0·32875	0·58739	0·0592	0·32784	0·5776	0·0592	0·34127	0·60689

Note: The second line of values corresponds to Sanders' theory, obtained by the authors, where the shear deformation effects are not taken into account.

TABLE 2

Comparison of lowest natural frequency parameters (empty, n=1)

	$[t/R]$			
$\lambda = m\pi R/L$	0·06	0·1	0·12	0·18
0·5π	0·01853	0·03101	0·03731	0·05656
	0·01853	0·03101	0·03730	0·05653
	0·01849	0·03099	0·03719	0·05649
	0·01853	0·03100	0·03730	0·05652
π	0·02782	0·04791	0·05872	0·09509
	0·02781	0·04785	0·05856	0·09409
	0·02780	0·04781	0·05835	0·09305
	0·02781	0·04784	0·05853	0·09402
2π	0·03717	0·07842	0·10517	0·20923
	0·03692	0·07615	0·10047	0·18832
	0·03690	0·07612	0·10010	0·18720
	0·03691	0·07618	0·10057	0·18894
4π	0·09161	0·23623	0·32960	0·67100
	0·08639	0·20478	0·27286	0·49818
	0·08616	0·20370	0·27210	0·49480
	0·08639	0·20529	0·27491	0·50338

Note: First row: Reference [17]; second row; Reference [18]; third row: present study; fourth row: Reference [19].

especially for $L/R > 2$. In fact, the part of the strain energy of a shell includes curvature effects, and couples the membrane and bending effects. In this case, the membrane effect is more significant than that of bending; see reference [14].

The non-dimensional frequency parameters (Ω) of an anisotropic empty shell (having symmetric $0^\circ/90^\circ/90^\circ/0^\circ$ layout) as a function of the radius-to-thickness ratio and axial

TABLE 3

Frequency parameter ($\Omega = \omega r\sqrt{\rho(1-\nu^2)/E}$) of a simply supported cylindrical shell (empty, n=0, m=1)

	$[R/t]$		
L/R	20	200	All values of R/t [20]
1	0·9647	0·9614	
	0·9483	0·9442	0·9489
2	0·9333	0·9331	
	0·9185	0·9183	0·9294
4	0·4666	0·4665	
	0·4548	0·4426	0·4646
6	0·3111	0·3110	
	0·3079	0·3077	0·3097
8	0·2333	0·2332	
	0·2224	0·2203	0·2323
9	0·2074	0·2074	
	0·2056	0·2051	0·2065
10	0·1866	0·1866	
	0·1849	0·1838	0·1859

Note: First row: Reference [10]; second row: present study.

TABLE 4

Non-dimensional natural frequency parameter ($\Omega = (\omega_0 R^2/t)\sqrt{\rho/E_2}$) of a symmetric cross-ply, 0°/90°/90°/0°, cylindrical shell (empty, L/R=5)

R/t	$[m]$							
	1		3		4		7	
	$n=0$	$n=1$	$n=0$	$n=1$	$n=0$	$n=1$	$n=0$	$n=1$
10	4·4044	3·0118	13·438	8·5781	18·017	11·278	21·767	21·484
	4·4551	3·0293	13·967	8·8159	18·057	12·251	31·364	30·413
20	8·8793	6·0226	21·814	15·175	26·296	18·896	35·473	34·428
	8·8951	6·0303	26·858	15·813	36·010	19·484	36·886	35·995
50	22·226	15·003	67·002	37·426	89·532	43·072	121·24	54·677
	22·234	15·152	67·243	39·845	90·471	46·904	159·23	62·852
100	44·466	30·004	100·15	74·420	122·13	84·810	132·665	98·780
	44·740	30·439	111·58	82·980	150·48	96·012	163·77	112·38

Note: The second line of values corresponds to Sanders' theory.

mode are given in Table 4 for axisymmetric and beam-like modes. The following material properties are used for this example: $E_1 = 25E_2$, $G_{23} = 0{\cdot}2E_2$, $G_{13} = G_{12} = 0{\cdot}5E_2$, $\nu_{12} = 0{\cdot}25$ and $\rho = 1$.

Table 5 shows the natural frequencies of an isotropic cylindrical shell simply supported at both ends, for both empty and fluid-filled cases, for the beam-like mode and the four first axial modes. The shell has the following properties: $R/t = 60$, $L/R = 24{\cdot}98$, $R = 0{\cdot}9\,\text{m}$, $\nu = 0{\cdot}3$, $E = 203{\cdot}4\,\text{GPa}$, $\rho_s = 7812\,\text{kg/m}^3$, $\rho_f = 1000\,\text{kg/m}^3$.

The results are listed along with those of Lakis and Sinno [10] and Niordson [15].

8.2. NATURAL VIBRATION OF THE PARTIALLY OR COMPLETELY FLUID-FILLED CYLINDRICAL SHELLS

In the case of vertical cylindrical shells, partially filled with liquid, it has been determined, by comparing the results of Lakis and Neagu [16] with those based on the theory presented by Lakis and Païdoussis [8], that the free surface effects are negligible for

TABLE 5

Free vibration (Hz) of a cylindrical shell simply supported at both ends (full and empty, $n = 1$)

m	Present	Niordson [15]	Lakis and Sinno [10]
1	9·5688	9·956	9·861
	4·1965	4·504	4·549
2	36·189	37·504	37·290
	16·062	17·257	17·46
3	75·042	77·271	77·900
	34·225	36·361	37·137
4	121·17	123·693	128·120
	55·63	59·594	62·115

Note: First line of values corresponds to empty shell; second line of values corresponds to fluid-filled shell.

TABLE 6

Frequency parameter ($\Omega = \omega r\sqrt{\rho(1-\nu^2)/E}$) of an isotropic cylindrical shell (full (empty) cases, n=1, m=1)

	[L/R]		
R/t	2	5	10
5	0·5304 (0·5867)	0·1674 (0·1860)	0·0526 (0·0592)
	0·4146 (0·5047)	0·1420 (0·1546)	0·0507 (0·0501)
10	0·4783 (0·5774)	0·1512 (0·1866)	0·0473 (0·0592)
	0·3728 (0·5136)	0·1442 (0·1856)	0·0460 (0·0551)
15	0·4442 (0·5767)	0·1391 (0·1865)	0·0433 (0·0592)
	0·3630 (0·5201)	0·1316 (0·1859)	0·0421 (0·0558)
20	0·4180 (0·5746)	0·1315 (0·1870)	0·0406 (0·0592)
	0·3356 (0·5416)	0·1220 (0·1826)	0·0393 (0·0572)
25	0·3958 (0·5792)	0·1218 (0·1866)	0·0377 (0·0592)
	0·3126 (0·5497)	0·1142 (0·1837)	0·0362 (0·0577)
30	0·3775 (0·5811)	0·1154 (0·1869)	0·0356 (0·0592)
	0·2944 (0·5508)	0·1077 (0·1847)	0·0344 (0·0580)
50	0·3219 (0·5770)	0·0983 (0·1875)	0·0300 (0·0592)
	0·2479 (0·5581)	0·0899 (0·1855)	0·0290 (0·0581)
100	0·2491 (0·5849)	0·0745 (0·1877)	0·0226 (0·0592)
	0·2002 (0·5601)	0·0684 (0·1872)	0·0219 (0·0582)
150	0·2244 (0·5924)	0·0635 (0·1876)	0·0189 (0·0592)
	0·1761 (0·5682)	0·0575 (0·1874)	0·0181 (0·0590)
200	0·1840 (0·5985)	0·0548 (0·1879)	0·0166 (0·0592)
	0·1590 (0·5776)	0·0506 (0·1875)	0·0161 (0·0592)

Note: The first line of values corresponds to Sanders' theory. The values in parantheses are related to empty case.

low frequencies (less than 3%), but may go up to 30% for modes higher than seven ($m \geqslant 7$). The principal cause of this phenomenon is attributed to the kinetic energy developed by the movement of the free surface; this effect diminishes the natural frequencies of the system as a function of the geometric and physical properties of the shell and of the axial and circumferential wave number. However, the potential energy due to the elevation of the wave has little effect on natural frequencies, because this energy is very small compared to the energy of deformation of the shell. On the other hand, the effect of the free surface is negligible at higher values of circumferential mode number ($n \geqslant 7$). The difference between frequencies calculated by the two methods (with and without free surface effects) is given by the difference of the kinetic energy developed by the free surface of the fluid versus the kinetic energy developed by the lateral surface of the fluid. Nevertheless, our aim in these calculations is to determine the effects of the shear deformation on the natural frequencies of anisotropic cylindrical shells.

The shear deformation effects on the non-dimensional natural frequencies of both fluid-filled and empty cylindrical shells for different values of L/R and R/t are given in Table 6

TABLE 7

Variation of non-dimensional frequency parameter ($\Omega = \omega r\sqrt{\rho(1-\nu^2)/E}$) of an isotropic, fluid-filled cylindrical shell as function of m and L/R (R/t=20, n=1)

L/R	m=1	m=2	m=3	m=5
1	0·6915	1·1133	1·5632	3·9925
	0·54463	1·1041	1·1458	2·4984
1·5	0·5338	0·85349	1·1133	1·8165
	0·41097	0·68841	1·1044	1·5863
2	0·4180	0·6915	0·91119	1·3173
	0·33555	0·54306	0·78549	1·1828
2·5	0·3314	0·62781	0·80636	1·1133
	0·27795	0·46211	0·63078	1·1107
3	0·2674	0·53380	0·6915	0·97203
	0·23195	0·41127	0·54253	0·96122
3·5	0·2195	0·47541	0·65894	0·88633
	0·19501	0·37087	0·48398	0·75834
4	0·1828	0·4180	0·59847	0·82434
	0·16536	0·33595	0·44397	0·66165
5	0·1315	0·3314	0·49715	0·6915
	0·12197	0·27821	0·38385	0·54210
6	0·0986	0·2674	0·4180	0·64627
	0·09281	0·23207	0·33608	0·47529
7	0·0762	0·21950	0·35468	0·57622
	0·07256	0·19510	0·29613	0·42941
8	0·0605	0·1828	0·30449	0·51551
	0·05805	0·16543	0·26175	0·39427
9	0·0491	0·15183	0·26740	0·46299
	0·04736	0·14148	0·23212	0·36356
10	0·0406	0·1315	0·23061	0·4180
	0·03930	0·12201	0·20656	0·33618

Note: The first line of values corresponds to Sanders' theory [10].

along with the corresponding results obtained from Sanders' theory. As can be seen, the influence of the transverse shear deformation on the natural frequencies is more pronounced for low values of L/R and R/t. One may observe that unshearable shell

TABLE 8

Variation of frequency parameter ($\Omega = \omega r\sqrt{\rho(1-\nu^2)/E}$) of an isotropic, fluid-filled cylindrical shell (m=1, n=1) as function of R/t and L/R

L/R	$[R/t]$				
	20	50	100	200	300
1	0·6915	0·5647	0·4621	0·3596	0·3018
	0·5446	0·3941	0·3415	0·3107	0·2425
1·5	0·5338	0·4214	0·3320	0·2485	0·2050
	0·4110	0·3062	0·2546	0·2123	0·1852
2	0·4180	0·3219	0·2491	0·1840	0·1519
	0·3356	0·2479	0·2002	0·1590	0·1354
2·5	0·3314	0·2525	0·1936	0·1426	0·1178
	0·2780	0·2049	0·1616	0·1247	0·1050
3	0·2674	0·2025	0·1546	0·1138	0·0941
	0·2320	0·1710	0·1327	0·1007	0·0842
3·5	0·2195	0·1665	0·1260	0·0927	0·0767
	0·1950	0·1435	0·1106	0·0830	0·0692
4	0·1828	0·1373	0·1044	0·0767	0·0635
	0·1654	0·1218	0·0933	0·0695	0·0578
5	0·1315	0·0983	0·0745	0·0548	0·0464
	0·1220	0·0899	0·0684	0·0506	0·0420
6	0·0986	0·0734	0·0556	0·0408	0·0337
	0·0928	0·0685	0·0519	0·0383	0·0317
7	0·0762	0·0566	0·0428	0·0314	0·0260
	0·0726	0·0536	0·0405	0·0298	0·0247
8	0·0605	0·0448	0·0339	0·0248	0·0205
	0·0581	0·0429	0·0324	0·0238	0·0197
9	0·0491	0·0363	0·0274	0·0201	0·0166
	0·0474	0·0349	0·0264	0·0194	0·0160
10	0·0406	0·0300	0·0226	0·0166	0·0137
	0·0393	0·0290	0·0219	0·0161	0·0133

Note: The first line of values corresponds to Sanders' theory [10].

TABLE 9

Non-dimensional natural frequency parameter ($\Omega = \omega_0 R^2/t\sqrt{\rho/E_2}$) of a symmetric cross-ply, 0°/90°90°/0°, cylindrical shell (fluid-filled, R/t=10)

L/R	m			
	1		3	
	$n=0$	$n=1$	$n=0$	$n=1$
1	10·982	9·9236	54·109	53·790
	18·280	13·91	79·817	78·850
5	4·4801	1·6079	5·8541	4·4643
	4·5607	1·6118	8·2140	5·4457

Note: The second line of values corresponds to Sanders' theory.

theory, in which the shear deformation effect is discarded, overestimates the frequencies for all parameters considered. Another conclusion to be drawn from this table is that the natural frequencies of the fluid-filled shell are lower than those of the corresponding empty shell due to increased kinetic energy of the system without a corresponding increase in the strain energy.

The next example, Table 7, shows the frequency variations of a fluid-filled simply supported cylindrical shell as a function of the axial mode number (m) and the length-to-radius ratio. The results obtained are compared with those of Sanders' theory.

It is noted that the eigenvalues for ($m = 1$ and $L/R = 1$), ($m = 2$ and $L/R = 2$), ($m = 3$ and $L/R = 3$), etc. as shown in Table 7, are quite similar. We find the following relationships for this example:

$$\Omega(m, L/R) = \begin{cases} \Omega(k, k') & \text{if } m \neq L/R, \\ \Omega(k, k) & \text{if } m = L/R, \end{cases}$$

$$k = m + i, i = 1, 2 \ldots \text{ and } k' = kL/R,$$

where Ω is the non-dimensional natural frequency. Thus, by knowing one of these values we may obtain some of the natural frequencies approximately.

Numerical results are presented in Table 8 for an isotropic fluid-filled cylindrical shell for different values of R/t and L/R ratios. The fluid contained in the shell is taken to be water. Comparing the results obtained from the present theory with those of Sanders' theory shows a significant difference for low values of R/t and L/R ratios. This means that the shear deformation effects are more pronounced for thicker and shorter shells.

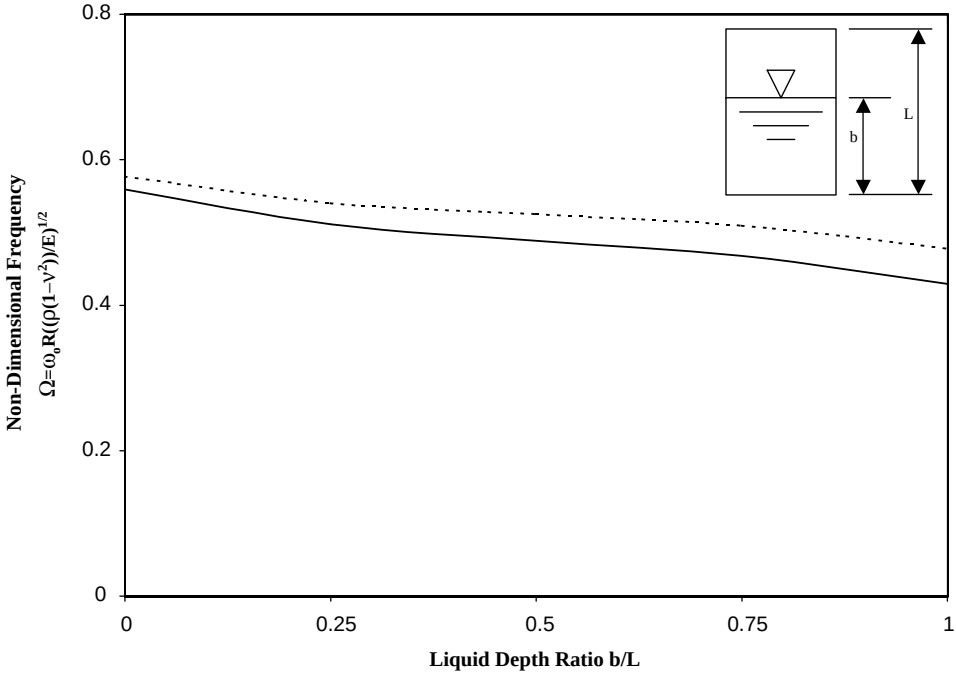

Figure 6. Variation of non-dimensional frequency of an isotropic fluid-filled cylindrical shell as variation of b/L. $R/t = 10$; $L/R = 2$; $n = 1$; $m = 1$; $E = 207\,\text{GPa}$; $\nu = 0{\cdot}3$; $\rho_s = 7812\,\text{kg/m}^3$; $\rho_f = 1000\,\text{kg/m}^3$. ——, Present theory; - - - - -, Sanders theory.

Table 9 presents the non-dimensional frequencies of an anisotropic, $0°/90°/90°/0°$ layout, fluid-filled shell for different values of axial modes (m) and L/R ratios, in cases of both axisymmetric and beam-like modes. The following materials are used in this example: $E_1 = 212\,\text{GPa}, E_2 = 12{\cdot}72\,\text{GPa}, G_{12} = 7{\cdot}42\,\text{GPa}, G_{13} = G_{23} = 0{\cdot}5G_{12}, \nu_{12} = \frac{1}{3}$.

The difference between the present theory and Sanders' shell theory is more pronounced in the case of anisotropic materials, as expected, due to the shear deformation effect.

The fluid depth effect is shown for isotropic and anisotropic shells in Figures 6 and 7. Figure 6 shows the effect for an isotropic cylindrical shell. All physical and geometrical parameters are given in the figure. Figure 7 shows the liquid depth effect on the natural frequencies of an antisymmetric cross-ply laminated cylindrical shell. The material properties used in this example are those in Table 9. As can be seen, the natural frequencies decrease considerably with increasing b/L.

8.3. NATURAL FREQUENCIES OF A CYLINDRICAL SHELL SUBJECTED TO A FLOWING FLUID

The stability of shells subjected to a flowing fluid is of practical importance because the natural frequency of structures generally decreases with the increasing velocity of fluid flow. The decrease in natural frequency can be important in certain problems involving very high-velocity flows through thin-walled structures, such as those used in the feed lines to rocket motors and water turbines. These structures may become susceptible to resonance or fatigue failure if their natural frequency falls below certain limits.

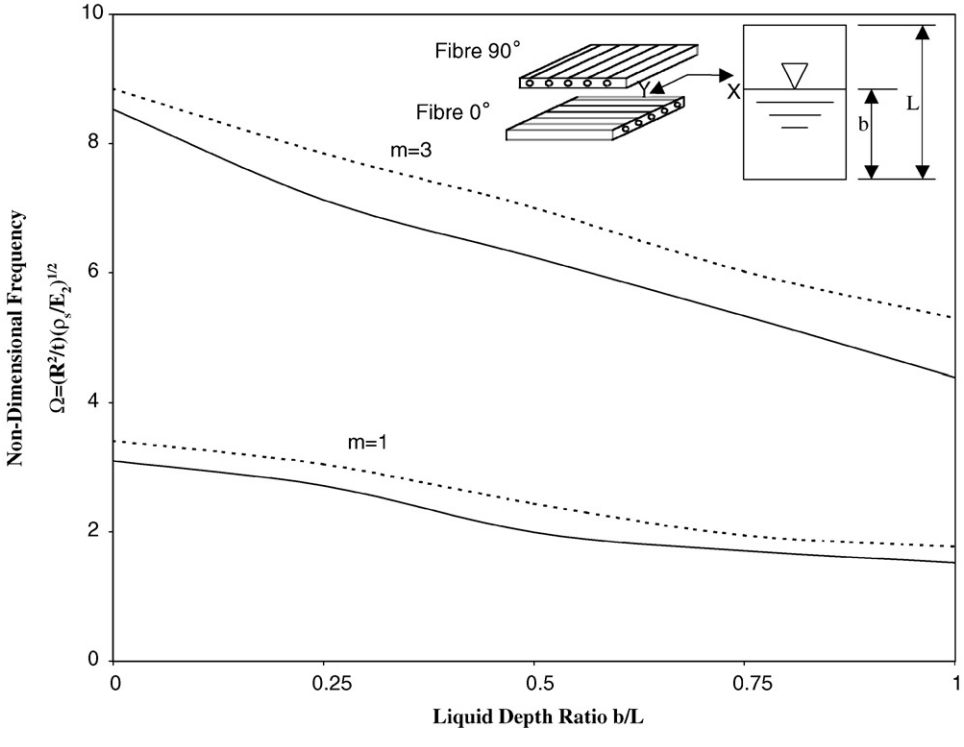

Figure 7. Variation of non-dimensional frequency parameter of an anisotropic laminated cylindrical shell ($0°/90°$) as a function of liquid depth ratio b/L and axial mode (m). $R/t = 10$; $L/R = 5$; $n = 1$. Key as in Figure 6.

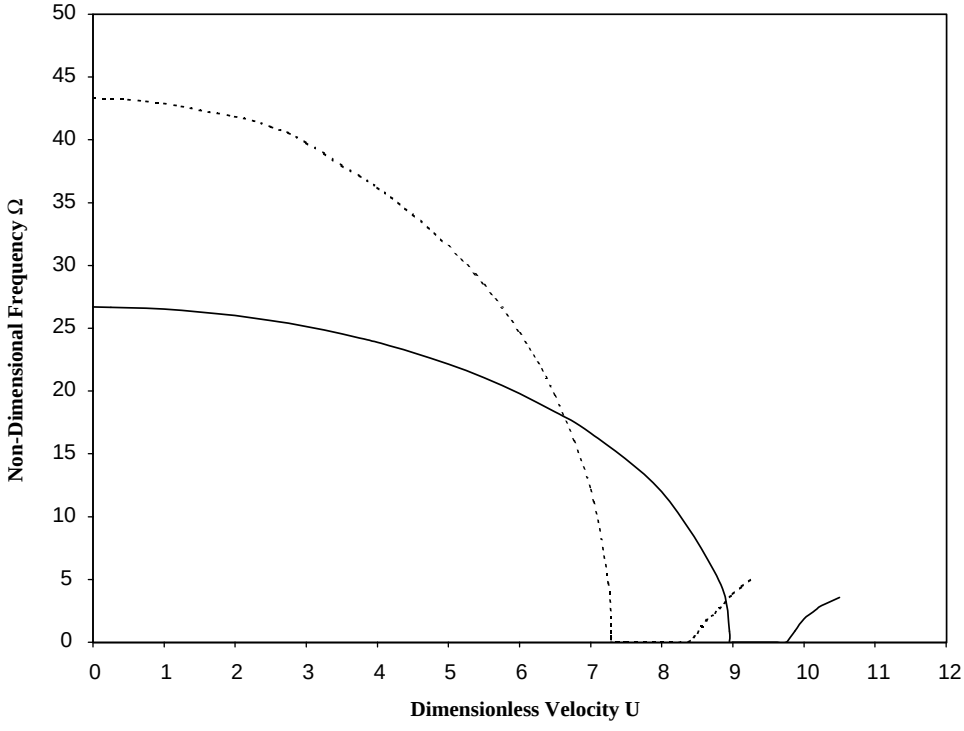

Figure 8. Stability of a simply supported cylindrical shell as a function of flow velocity (internal flow). $\Omega = \omega/\omega_0$; $U = u/u_0$; $\omega_0 = (\pi^2/L^2)/(K/\rho_s t)^{1/2}$; $u_0 = \omega_0 L$; $K = Et^3/12(1\text{-}\nu^2)$; $\rho_f/\rho_s = 0{\cdot}128$; $L/R = 2$; $n = 1$. ——, $m = 1, R/t = 50$; - - - - -, $m = 2, R/t = 100$.

The influence of the internal flow velocity on the non-dimensional natural frequency parameter of an isotropic cylindrical shell is shown in Figure 8 for the case of the beam-like mode. All parameters are given in the figure. The 'u' and ω are, respectively, the velocity of the flowing fluid and the natural frequency.

It is observed that the frequencies associated with both modes decrease as the fluid velocity increases from zero. The frequency parameters remain real (the system being conservative) until they vanish at high velocities, indicating the existence of a static divergence instability (where $\Omega = 0$). In this case, the frequencies become purely imaginary.

Also, it can be seen from this figure that the dimensionless critical flow velocity increases as thickness-to-radius ratio and axial mode number increase. If the velocity is increased further, the natural frequencies for both cases reappear and would coalesce with those of the following mode numbers to produce coupled mode flutter.

9. CONCLUSIONS

An analytical procedure has been developed for determining the natural vibration frequencies of the anisotropic cylindrical shells conveying fluid. The hybrid formulation used in this paper has its basis in the finite element method, but with the displacement functions over an element determined by the *exact* solution of equilibrium equations of the thin cylindrical shells (shearable shell theory) instead of the usual and more arbitrary

interpolation polynomials. In doing so, the accuracy of the formulations is less affected as the number of elements used is decreased (thus reducing computation time) and as the dynamic characteristics of the shell are required at higher beam-mode number (m) or higher shell-mode number (n), a significant advantage over polynomial interpolations. Moreover, this formulation allows for convenient axial modelling in the case of axially non-uniform shells.

Only, the *axisymmetric* ($n = 0$) and *beam-like* ($n = 1$) cases have been considered in this paper. In the axisymmetric case, two systems of displacement functions are derived for the torsional and non-torsional motions.

The shape functions are derived by analytical integration, from the *exact* solution of shearable shell equations. Thereafter, the mass and stiffness matrices of each structural element are derived by exact analytical integration. The fluid pressure is analytically integrated over the liquid element to obtain the mass, stiffness and damping matrices due to the fluid effect.

The results obtained from this theory are compared with those of non-shearable shell theory and other available results. The following conclusions may be drawn: (1) shear deformation effect is more pronounced for anisotropic shells and increases with increasing the shell thickness, (2) the natural frequencies of fluid–filled shells are lower than the corresponding values of empty shells due to increased kinetic energy of the system without a corresponding increase in strain energy, (3) depending on boundary conditions, the fluid-shell systems may experience a loss of static (buckling) or dynamic (flutter) stability when the flow velocity reaches high enough values, (4) longer shells lose their stability in the beam mode ($m = 1, n = 1$) while the lowest mode of instabilities becomes shell related as L/R decreases.

REFERENCES

1. L. Librescu 1975 *Elastostatics and Kinetics of Anisotropic and Heterogeneous Shell-type Structures*. Leyden, Netherlands: Noordhoff International Publishing.
2. M. H. Toorani and A. A. Lakis 2000 *Journal of Sound and Vibration* **237**, 561–615. General equations of anisotropic plates and shells including transverse shear deformations, rotary inertia and initial curvature effects.
3. H. Lamb 1945 *Hydrodynamics*. New York: Dover; sixth edition.
4. M. P. Païdoussis 1998 *Fluid–Structure Interactions, Slender Structures and Axial Flow*, Vol. I. New York: Academic Press.
5. R. D. Blevin 1990 Flow-Induced Vibration. Malabar, FL: Robert E. Krieger Publishing Company, Inc.
6. H. N. Abramson 1966 *NASA SP*-106. The dynamic behavior of liquids in moving containers.
7. H. J. P. Morand and R. Ohayon 1995 *Interactions Fluids–Structures*. New York: John Wiley.
8. A. A. Lakis and M. P. Païdoussis 1971 *Journal of Sound and Vibration* **19**, 1–15. Free vibration of cylindrical shells partially filled with liquid.
9. J. L. Sanders 1959 *NASA*, TR R-24, 1–23. An improved first approximation theory for thin shells.
10. A. A. Lakis and M. Sinno 1992 *International Journal for Numerical Methods in Engineering* **33**, 235–268. Free vibration of axisymmetric and beam-like cylindrical shells partially filled with liquid.
11. A. Selamne and A. A. Lakis 1997 *Journal of Fluid and Structures* **11**, 111–134. Vibration analysis of anisotropic open cylindrical shells subjected to a flowing fluid.
12. M. H. Toorani, A. A. Lakis and M. Amabili 2000 *Fourth International Colloquium on Computation of Shell & Spatial Structures, IASS-IACM* 2000, *Chania-Crete, Greece*, June. Dynamics behavior of anisotropic shells including transverse shear deformation and rotary inertia effects.
13. M. H. Toorani and A. A. Lakis 2000 *Eighth International Conference on Nuclear Engineering ICONE8, Baltimore, MD, U.S.A.* April. Transverse shear deformation in dynamics behavior of anisotropic laminated piping subjected to a flowing fluid.

14. C. D. MICHALOPOULOS and D. MUSTER 1967 in *Proceedings of the Symposium on the Theory of Shells, University of Houston*, D. Muster editor. 345. The in-vacuo vibrations of simply supported ring-stiffened mass-loaded cylindrical shells.
15. F. I. N. NIORDSON 1953 *Transactions of the Royal Institute of Technology (Stockholm)* **3**, p. 73. Vibration of a cylindrical tube containing flowing fluid.
16. A. A. LAKIS and S. NEAGU 1997 *Journal of Sound and Vibration* **207**, 175–205. Free surface effects on the dynamics of cylindrical shells partially filled with liquid.
17. W. FLÜGGE 1962 *Stresses in Shells*. Berlin: Springer-Verlag.
18. A. BHIMARDDI 1984 *International Journal of Solids and Structures* **20**, 623–630. A higher order theory for free vibration analysis of circular cylindrical shells.
19. A. E. ARMENÀKAS and D. GAZIS and G. HERRMANN 1969 *Free Vibration of Circular Cylindrical Shells*. Oxford: Pergamon Press.
20. M. L. BARON and H. H. BLEICH 1954 *Journal of Applied Mechanics American Society of Mechanical Engineers* **21**, 178. Tables of frequencies and modes of free vibration of infinitely long thin cylindrical shell.

APPENDIX A: EQUATIONS OF MOTION

Appendix A gives the differential equations of motion for two cases ($n = 1$, beam-like and $n = 0$, axisymmetric).

A.1. THE EQUATIONS OF MOTION OF A CYLINDRICAL SHELL (EQUATION (4) FOR CASE $\mathbf{n} = 1$)

$$\begin{aligned}
&L_1^1(U, V, W, \beta_x, \beta_\theta, \overline{P_{ij}}) \\
&\quad = P_{11}\frac{\partial^2 U}{\partial x^2} + \left(\frac{1}{R}(P_{15} + P_{51})\right)\frac{\partial^2 U}{\partial x \partial \theta} + \left(\frac{P_{55}}{R^2}\right)\frac{\partial^2 U}{\partial \theta^2} - I_1\frac{\partial^2 U}{\partial t^2} + (P_{12})\frac{\partial^2 V}{\partial x^2} \\
&\qquad + \left(\frac{1}{R}(P_{14} + P_{52})\right)\frac{\partial^2 V}{\partial x \partial \theta} + \left(\frac{P_{54}}{R^2}\right)\frac{\partial^2 V}{\partial \theta^2} + \frac{P_{14}}{R}\frac{\partial W}{\partial x} + \left(\frac{P_{54}}{R^2}\right)\frac{\partial W}{\partial \theta} \\
&\qquad + P_{17}\frac{\partial^2 \beta_x}{\partial x^2} + \left(\frac{1}{R}(P_{1,10} + P_{57})\right)\frac{\partial^2 \beta_x}{\partial x \partial \theta} + \left(\frac{P_{5,10}}{R^2}\right)\frac{\partial^2 \beta_x}{\partial \theta^2} - I_2\frac{\partial^2 \beta_x}{\partial t^2} \\
&\qquad + P_{18}\frac{\partial^2 \beta_\theta}{\partial x^2} + \left(\frac{1}{R}(P_{19} + P_{58})\right)\frac{\partial^2 \beta_\theta}{\partial x \partial \theta} + \left(\frac{P_{59}}{R^2}\right)\frac{\partial^2 \beta_\theta}{\partial \theta^2},
\end{aligned} \tag{A.1}$$

$$\begin{aligned}
L_2^1(U, V, W, \beta_x, \beta_\theta, \overline{P_{ij}}) &= (P_{21})\frac{\partial^2 U}{\partial x^2} + \left(\frac{1}{R}(P_{25} + P_{41})\right)\frac{\partial^2 U}{\partial x \partial \theta} + \left(\frac{P_{45}}{R^2}\right)\frac{\partial^2 U}{\partial \theta^2} \\
&\quad + (P_{22})\frac{\partial^2 V}{\partial x^2} + \left(\frac{1}{R}(P_{24} + P_{42})\right)\frac{\partial^2 V}{\partial x \partial \theta} + \frac{P_{44}}{R^2}\frac{\partial^2 V}{\partial \theta^2} \\
&\quad - \frac{P_{66}}{R^2}V - I_1\frac{\partial^2 V}{\partial t^2} + \left(\frac{1}{R}(P_{24} + P_{63})\right)\frac{\partial W}{\partial x} + \frac{1}{R^2}(P_{44} + P_{66})\frac{\partial W}{\partial \theta} \\
&\quad + (P_{27})\frac{\partial^2 \beta_x}{\partial x^2} + \left(\frac{1}{R}(P_{2,10} + P_{47})\right)\frac{\partial^2 \beta_x}{\partial x \partial \theta} + \frac{P_{4,10}}{R^2}\frac{\partial^2 \beta_x}{\partial \theta^2} + \frac{P_{63}}{R}\beta_x \\
&\quad + (P_{28})\frac{\partial^2 \beta_\theta}{\partial x^2} + \left(\frac{1}{R}(P_{29} + P_{48})\right)\frac{\partial^2 \beta_\theta}{\partial x \partial \theta} + \frac{P_{49}}{R^2}\frac{\partial^2 \beta_\theta}{\partial \theta^2} \\
&\quad + \frac{P_{66}}{R}\beta_\theta - I_2\frac{\partial^2 \beta_\theta}{\partial t^2},
\end{aligned} \tag{A.2}$$

$$L_3^1(U,V,W,\beta_x,\beta_\theta,\overline{P_{ij}}) = -\frac{P_{41}}{R}\frac{\partial U}{\partial x} - \left(\frac{P_{45}}{R^2}\right)\frac{\partial U}{\partial \theta} - \frac{1}{R}(P_{36}+P_{42})\frac{\partial V}{\partial x} - \frac{1}{R^2}(P_{44}+P_{66})\frac{\partial V}{\partial \theta} + P_{33}\frac{\partial^2 W}{\partial x^2} + \frac{1}{R}(P_{63}+P_{36})\frac{\partial^2 W}{\partial x \partial \theta} + \frac{P_{66}}{R^2}\frac{\partial^2 W}{\partial \theta^2} - \frac{P_{44}}{R^2}W - I_1\frac{\partial^2 W}{\partial t^2} + (P_{33})\frac{\partial \beta_x}{\partial x} + \frac{1}{R}(P_{63})\frac{\partial \beta_x}{\partial \theta} + (P_{36})\frac{\partial \beta_\theta}{\partial x} + \frac{1}{R}(P_{66})\frac{\partial \beta_\theta}{\partial \theta}, \tag{A.3}$$

$$L_4^1(U,V,W,\beta_x,\beta_\theta,\overline{P_{ij}}) = P_{71}\frac{\partial^2 U}{\partial x^2} + \left(\frac{1}{R}(P_{75}+P_{10,1})\right)\frac{\partial^2 U}{\partial x \partial \theta} + \left(\frac{P_{10,5}}{R^2}\right)\frac{\partial^2 U}{\partial \theta^2} - I_2\frac{\partial^2 U}{\partial t^2} + (P_{72})\frac{\partial^2 V}{\partial x^2} + \left(\frac{1}{R}(P_{74}+P_{10,2})\right)\frac{\partial^2 V}{\partial x \partial \theta} + \frac{P_{10,4}}{R^2}\frac{\partial^2 V}{\partial \theta^2} + \frac{P_{36}}{R}V - (P_{33})\frac{\partial W}{\partial x} - \left(\frac{P_{36}}{R}\right)\frac{\partial W}{\partial \theta} + P_{77}\frac{\partial^2 \beta_x}{\partial x^2} + \frac{1}{R}(P_{7,10}+P_{10,7})\frac{\partial^2 \beta_x}{\partial x \partial \theta} + \frac{P_{10,10}}{R^2}\frac{\partial^2 \beta_x}{\partial \theta^2} - P_{33}\beta_x - I_3\frac{\partial^2 \beta_x}{\partial t^2} + P_{78}\frac{\partial^2 \beta_\theta}{\partial x^2} + \frac{1}{R}(P_{79}+P_{10,8})\frac{\partial^2 \beta_\theta}{\partial x \partial \theta} + \frac{P_{10,9}}{R^2}\frac{\partial^2 \beta_\theta}{\partial \theta^2} - P_{36}\beta_\theta, \tag{A.4}$$

$$L_5^1(U,V,W,\beta_x,\beta_\theta,\overline{P_{ij}}) = P_{81}\frac{\partial^2 U}{\partial x^2} + \left(\frac{1}{R}(P_{85}+P_{91})\right)\frac{\partial^2 U}{\partial x \partial \theta} + \left(\frac{P_{95}}{R^2}\right)\frac{\partial^2 U}{\partial \theta^2} + (P_{82})\frac{\partial^2 V}{\partial x^2} + \left(\frac{1}{R}(P_{84}+P_{92})\right)\frac{\partial^2 V}{\partial x \partial \theta} + \frac{P_{94}}{R^2}\frac{\partial^2 V}{\partial \theta^2} + \frac{P_{66}}{R}V - I_2\frac{\partial^2 V}{\partial t^2} - (P_{63})\frac{\partial W}{\partial x} - \left(\frac{P_{66}}{R}\right)\frac{\partial W}{\partial \theta} + P_{87}\frac{\partial^2 \beta_x}{\partial x^2} + \frac{1}{R}(P_{97}+P_{8,10})\frac{\partial^2 \beta_x}{\partial x \partial \theta} - P_{63}\beta_x + \frac{P_{9,10}}{R^2}\frac{\partial^2 \beta_x}{\partial \theta^2} + P_{88}\frac{\partial^2 \beta_\theta}{\partial x^2} + \frac{1}{R}(P_{89}+P_{98}) \times \frac{\partial^2 \beta_\theta}{\partial x \partial \theta} + \frac{P_{99}}{R^2}\frac{\partial^2 \beta_\theta}{\partial \theta^2} - P_{66}\beta_\theta - I_3\frac{\partial^2 \beta_\theta}{\partial t^2}. \tag{A.5}$$

A.2. THE EQUATIONS OF MOTION OF A CYLINDRICAL SHELL (EQUATION (4) FOR CASE $\mathbf{n} = 0$)

$$L_1^0(U,V,W,\beta_x,\beta_\theta,\overline{P_{ij}}) = P_{11}\frac{\partial^2 U}{\partial x^2} - I_1\frac{\partial^2 U}{\partial t^2} + \frac{P_{14}}{R}\frac{\partial W}{\partial x} + P_{17}\frac{\partial^2 \beta_x}{\partial x^2} - I_2\frac{\partial^2 \beta_x}{\partial t^2}, \tag{A.6}$$

$$L_2^0(U,V,W,\beta_x,\beta_\theta,\overline{P_{ij}}) = \left(\frac{P_{82}}{2R} + \frac{P_{88}}{4R^2} + P_{22} + \frac{P_{28}}{R}\right)\frac{\partial^2 V}{\partial x^2} - \frac{P_{66}}{R^2}V - I_1\frac{\partial^2 V}{\partial t^2} + \left(\frac{P_{88}}{2R} + P_{28}\right)\frac{\partial^2 \beta_\theta}{\partial x^2} + \frac{P_{66}}{R}\beta_\theta - I_2\frac{\partial^2 \beta_\theta}{\partial t^2}, \tag{A.7}$$

$$L_3^0(U, V, W, \beta_x, \beta_\theta, \overline{P_{ij}}) = -\frac{P_{41}}{R}\frac{\partial U}{\partial x} + P_{33}\frac{\partial^2 W}{\partial x^2} - \frac{P_{44}}{R^2}W - I_1\frac{\partial^2 W}{\partial t^2} + \left(P_{33} - \frac{P_{47}}{R}\right)\frac{\partial \beta_x}{\partial x}, \tag{A.8}$$

$$L_4^0(U, V, W, \beta_x, \beta_\theta, \overline{P_{ij}}) = P_{71}\frac{\partial^2 U}{\partial x^2} - I_2\frac{\partial^2 U}{\partial t^2} + \left(\frac{P_{74}}{R} - P_{33}\right)\frac{\partial W}{\partial x} + P_{77}\frac{\partial^2 \beta_x}{\partial x^2} - P_{33}\beta_x - I_3\frac{\partial^2 \beta_x}{\partial t^2}, \tag{A.9}$$

$$L_5^0(U, V, W, \beta_x, \beta_\theta, \overline{P_{ij}}) = \left(P_{82} + \frac{P_{88}}{2R}\right)\frac{\partial^2 V}{\partial x^2} + \frac{P_{66}}{R}V - I_2\frac{\partial^2 V}{\partial t^2} + P_{88}\frac{\partial^2 \beta_\theta}{\partial x^2} - P_{66}\beta_\theta - I_3\frac{\partial^2 \beta_\theta}{\partial t^2}. \tag{A.10}$$

APPENDIX B: EQUATIONS OF THE BEAM-LIKE CASE

Appendix B is related to the corresponding equations of the beam-like case ($\mathbf{n} = 1$). The elements of matrix $[T]$ given in equation (5) are

$$[T] = \begin{bmatrix} \cos\theta & 0 & 0 & 0 & 0 \\ 0 & \sin\theta & 0 & 0 & 0 \\ 0 & 0 & \cos\theta & 0 & 0 \\ 0 & 0 & 0 & \cos\theta & 0 \\ 0 & 0 & 0 & 0 & \sin\theta \end{bmatrix}. \tag{B.1}$$

The elements of matrix $[H_1]$ given in equation (6) are

$$\begin{aligned}
&h_{11} = P_{11}\lambda^2 - (P_{15} + P_{51})\lambda - P_{55}, \quad h_{12} = P_{12}\lambda^2 + (P_{14} + P_{52})\lambda - P_{54},\\
&h_{13} = P_{14}\lambda - P_{54}, \quad h_{14} = P_{17}\lambda^2 - \left(P_{1,10} + P_{57}\right)\lambda - P_{5,10},\\
&h_{15} = P_{18}\lambda^2 + (P_{19} + P_{58})\lambda - P_{59}, \quad h_{22} = P_{22}\lambda^2 + (P_{24} + P_{42})\lambda - (P_{44} + P_{66}),\\
&h_{23} = (P_{24} + P_{63})\lambda - (P_{44} + P_{66}), \quad h_{24} = P_{27}\lambda^2 - \left(P_{2,10} + P_{47}\right)\lambda - (P_{4,10} - RP_{63}),\\
&h_{25} = P_{28}\lambda^2 + (P_{29} + P_{48})\lambda - (P_{49} - RP_{66}), \quad h_{33} = P_{33}\lambda^2 - (P_{36} + P_{63})\lambda - (P_{44} + P_{66}),\\
&h_{34} = R(P_{33}\lambda - P_{63}), \quad h_{35} = R(P_{36}\lambda + P_{66}),\\
&h_{44} = P_{77}\lambda^2 - \left(P_{7,10} + P_{10,7}\right)\lambda - (P_{10,10} + R^2P_{33}),\\
&h_{45} = P_{78}\lambda^2 + \left(P_{79} + P_{10,8}\right)\lambda - (P_{10,9} + R^2P_{36}),\\
&h_{55} = P_{88}\lambda^2 + (P_{89} + P_{98})\lambda - (P_{99} + R^2P_{66}).
\end{aligned} \tag{B.2}$$

The elements of matrix $[R_1]$ given in equation (9) are

$$\begin{aligned}
&R_1(1, i) = \alpha_i a_i, \quad R_1(2, i) = \beta_i a_i, \quad R_1(3, i) = a_i,\\
&R_1(4, i) = \gamma_i a_i, \quad R_1(5, i) = \delta_i a_i,\\
&\text{where } a_i = \lambda_i(x/R) \text{ and } i = 1, 2, \ldots, 10.
\end{aligned} \tag{B.3}$$

The elements of matrix $[A_1]$ given in equation (11) are

$$A_1(1,i)=\alpha_i,\quad A_1(6,i)=\alpha_i a_i,\quad A_1(2,i)=\beta_i,\quad A_1(7,i)=\beta_i a_i,$$
$$A_1(3,i)=1,\quad A_1(8,i)=a_i,\quad A_1(4,i)=\gamma_i,\quad A_1(9,i)=\gamma_i a_i,$$
$$A_1(5,i)=\delta_i,\quad A_1(10,i)=\delta_i a_i, \tag{B.4}$$

where $a_i=\lambda_i(x/R)$ and $i=1,2,\ldots,10$.

The elements of matrix $[Q_1]$ given in equation (23) are

$$Q_1(1,i)=A_i a_i,\quad Q_1(6,i)=F_i a_i,\quad Q_1(2,i)=B_i a_i,\quad Q_1(7,i)=G_i a_i,$$
$$Q_1(3,i)=C_i a_i,\quad Q_1(8,i)=H_i a_i,\quad Q_1(4,i)=D_i a_i,\quad Q_1(9,i)=I_i a_i,$$
$$Q_1(5,i)=E_i a_i,\quad Q_1(10,i)=J_i a_i, \tag{B.5}$$

where

$$A_i=\tfrac{\lambda_i}{R}\alpha_i,\quad F_i=\tfrac{-1}{R}(1+\beta_i)+\delta_i,\quad B_i=\tfrac{\lambda_i}{R}\beta_i,\quad G_i=\tfrac{\lambda_i}{R}\gamma_i,$$
$$C_i=\tfrac{\lambda_i}{R}+\gamma_i,\quad H_i=\tfrac{\lambda_i}{R}(\delta_i+\tfrac{1}{2R}\beta_i),$$
$$D_i=\tfrac{1}{R}(\beta_i+1),\quad I_i=\tfrac{1}{R}\delta_i,\quad E_i=\tfrac{-1}{R}\alpha_i,\quad J_i=\tfrac{-1}{R}(\gamma_i-\tfrac{1}{2R}\alpha_i), \tag{B.6}$$

and $a_i=\lambda x/R$ and $i=1,2,\ldots,10$.

The parameters given in equations (27) and (28) are

$$\begin{aligned}\Gamma_1(i,j)&=(\alpha_i\alpha_j+\beta_i\beta_j+1+\gamma_i\gamma_j+\delta_i\delta_j),\\ \Pi_1(i,j)&=[P_{11}A_iA_j+P_{14}A_iD_j+P_{17}A_iG_j+P_{19}A_iI_j\\ &\quad+P_{22}B_iB_j+P_{25}B_iE_j+P_{28}B_iH_j+P_{2,10}B_iJ_j\\ &\quad+P_{33}C_iC_j\\ &\quad+P_{41}D_iA_j+P_{44}D_iD_j+P_{47}D_iG_j+P_{49}D_iI_j\\ &\quad+P_{52}E_iB_j+P_{55}E_iE_j+P_{58}E_iH_j+P_{5,10}E_iJ_j\\ &\quad+P_{66}F_iF_j\\ &\quad+P_{71}G_iA_j+P_{74}G_iD_j+P_{77}G_iG_j+P_{79}G_iI_j\\ &\quad+P_{82}H_iB_j+P_{85}H_iE_j+P_{88}H_iH_j+P_{8,10}H_iJ_j\\ &\quad+P_{91}I_iA_j+P_{94}I_iD_j+P_{97}I_iG_j+P_{99}I_iI_j+\\ &\quad+P_{10,2}J_iB_j+P_{10,5}J_iE_j+P_{10,8}J_iH_j+P_{10,10}J_iJ_j],\\ &\quad i,j=1,2,\ldots,10.\end{aligned} \tag{B.7}$$

APPENDIX C: EQUATIONS OF THE AXISYMMETRIC CASE

Appendix C is related to corresponding equations of axisymmetric case ($\mathbf{n}=0$).

C.1. NON-TORSIONAL CASE

The elements of matrix $[H_0]$ defined in equation (14) are

$$h^0_{11}=P_{11}\lambda^2,\quad h^0_{12}=P_{14}\lambda,\quad h^0_{13}=P_{17}\lambda^2,$$
$$h^0_{22}=P_{33}\lambda^2-P_{44},\quad h^0_{23}=(RP_{33}-P_{47})\lambda,$$
$$h^0_{33}=P_{77}\lambda^2-R^2P_{33}. \tag{C.1}$$

The coefficients of polynomial equation (15) are

$$\begin{aligned} f_6^0 &= P_{11}P_{33}P_{77} - P_{17}^2P_{33}, \\ f_4^0 &= P_{11}P_{47}^2 + P_{44}P_{17}^2 + P_{77}P_{14}^2 \\ &\quad + 2P_{14}P_{71}(RP_{33} - P_{47}) - P_{11}(P_{44}P_{77} + 2RP_{47}P_{33}), \\ f_2^0 &= R^2P_{33}(P_{11}P_{44} - P_{14}^2). \end{aligned} \tag{C.2}$$

The elements of matrix $[R_0]$ given in equation (16) are

$$\begin{aligned} &R_0(1,i) = \alpha_i e^{\lambda_i x/R}, R_0(2,i) = e^{\lambda_i x/R}, \\ &R_0(3,i) = \gamma_i e^{\lambda_i x/R}, i = 1{-}6. \end{aligned} \tag{C.3}$$

The elements of $[A_0]$ given in equation (17) are

$$\begin{aligned} &A_0(1,i) = \alpha_i, \quad A_0(2,i) = 1, \quad A_0(3,i) = \gamma_i, \\ &A_0(4,i) = \alpha_i a_i, \quad A_0(5,i) = a_i, \quad A_0(6,i) = \gamma_i a_i, \end{aligned} \tag{C.4}$$

where $a_i = e^{\lambda_i \ell/R}$ and $i = 1{-}6$.

The strain vector for the non-torsional case for the axisymmetric mode ($\mathbf{n} = 0$), equation (29), is

$$\{\varepsilon_0\} = \begin{Bmatrix} \varepsilon_x^0 \\ \mu_x^0 \\ \varepsilon_\theta^o \\ \kappa_x \end{Bmatrix} = \begin{Bmatrix} \dfrac{\partial U}{\partial x} \\ \dfrac{\partial W}{\partial x} + \beta_x \\ \dfrac{W}{R} \\ \dfrac{\partial \beta_x}{\partial x} \end{Bmatrix}. \tag{C.5}$$

The elements of matrix $[Q_0]$ given in equation (29) are

$$\begin{aligned} &Q_0(1,i) = a_i\alpha_i e^{\lambda_i x/R}, Q_0(2,i) = (a_i + \gamma_i)e^{\lambda_i x/R}, \\ &Q_0(3,i) = \frac{1}{R}e^{\lambda_i x/R}, Q_0(4,i) = a_i\gamma_i e^{\lambda_i x/R}, \\ &\text{where } a_i = \lambda_i/R \text{ and } i = 1{-}6. \end{aligned} \tag{C.6}$$

The parameters given in equation (31) are

$$\begin{aligned} &\Gamma_0(i,j) = \left(\alpha_i\alpha_j + 1 + \gamma_i\gamma_j\right), \\ &\Pi_0(i,j) = \begin{bmatrix} P_{11}A_iA_j + \dfrac{P_{14}}{R}A_i + P_{17}A_iG_j + P_{33}C_iC_j + \dfrac{P_{41}}{R}A_j \\ +\dfrac{P_{44}}{R^2} + \dfrac{P_{47}}{R}G_j + P_{71}G_iA_j + \dfrac{P_{74}}{R}G_i + P_{77}G_iG_j \end{bmatrix}, \quad i,\ j = 1,2,...,6. \end{aligned} \tag{C.7}$$

C.2. TORSIONAL CASE

The elements of matrix $\left[A_0'\right]$ given in equation (21) are

$$\begin{aligned} A_0'(1,1) = A_0'(2,2) = A_0'(3,1) = A_0'(4,2) = 1, \\ A_0'(3,3) = A_0'(4,4) = \ell, \text{other terms} = 0. \end{aligned} \tag{C.8}$$

The elements of matrix $[R'_0]$ given in equation (21) are

$$R'_0(1,1) = R'_0(2,2) = 1, R'_0(1,3) = R'_0(2,4) = x, \text{other terms} = 0. \tag{C.9}$$

The strain vector of the torsional case for the axisymmetric mode ($\mathbf{n} = 0$), equation (32), is

$$\{\varepsilon'_0\} = \begin{Bmatrix} \gamma_x^0 \\ \mu_\theta^0 \\ \tau_x \end{Bmatrix} = \begin{Bmatrix} \dfrac{\partial V}{\partial x} \\ -\dfrac{V}{R} + \beta_\theta \\ \dfrac{\partial \beta_\theta}{\partial x} + \dfrac{1}{2R}\dfrac{\partial V}{\partial x} \end{Bmatrix}. \tag{C.10}$$

The elements of matrix $[Q'_0]$ given in equation (32) are

$$\begin{aligned} &Q'_0(1,1) = Q'_0(1,2) = Q'_0(1,4) = Q'_0(3,1) = Q'_0(3,2) = 0, \\ &Q'_0(1,3) = Q'_0(2,2) = Q'_0(3,4) = 1, Q'_0(2,4) = x, \\ &Q'_0(2,1) = -1/R, Q'_0(2,3) = xQ'_0(2,1), Q'_0(3,3) = -\tfrac{1}{2}Q'_0(2,1). \end{aligned} \tag{C.11}$$

APPENDIX D: PARAMETER USED IN EQUATION (53)

Appendix D is given for the parameter defined in section 6.3. The parameter used in equation (53) is

$$\Xi_{kq} = \begin{cases} \dfrac{1}{(\lambda_k + \lambda_q)}\left[e^{(\lambda_k+\lambda_q)\ell/R_{i,e}} - 1\right] & \text{if } \lambda_k + \lambda_q \neq 0, \\ \dfrac{\ell}{R_{i,e}} & \text{if } \lambda_k + \lambda_q = 0. \end{cases} \tag{D.1}$$

APPENDIX E: NOMENCLATURE

A, B, C, D, E	defined by equation (5)
$A_i, B_i, C_i, \ldots, J_I$	defined by equation (B.6)
B_0, B_1	given in equation (20)
E_0, E_1	given in equation (20)
f_i and f_i^o	coefficients of characteristic equations (7) and (15)
i	$i^2 = -1$
$J_{nj}(im_j r)$	Bessel function of the first kind and of order n
ℓ	length of element
L	length of shell
L_I	equations of motion (4)
m	axial mode number
$M_x, M_\theta, M_{x\theta}, M_{\theta x}$	the resultant moments (3)
N	circumferential wave number
$N_x, N_\theta, N_{x\theta}, N_{\theta x}$	the resultant in-plane forces (3)
P	lateral pressure exerted on the shell
P_i	internal pressure
P_e	external pressure
$Q_{xx}, Q_{\theta\theta}$	the resultant transverse forces equation (3)
R	mean radius of the shell
$R_j(r)$	solution of Bessel equation (45)
$S_j(x, \theta, t)$	defined by equation (43)
t	thickness of the shell

u, v, w	the axial, circumferential and radial displacements respectively
$U, V, W, \beta_x, \beta_\theta$	amplitudes of u, v, w, β_x and β_θ
U_x	velocity of the fluid, i internal fluid and e external fluid
V_x, V_θ, V_r	axial, tangential and radial fluid velocities (38)
x	axial co-ordinate
$Y_{nj}(im_j r)$	Bessel function of the second kind and of order n
$Z_j(im_j R_j)$	defined by equation (49)
$\alpha_i, \beta_i, \gamma_i$ and δ_i	defined by equation (8)
β_x and β_θ	the rotations of tangents to the reference surface
λ	complex roots of the characteristic equation (7)
ε_x^0 and ε_θ^0	normal strains of the reference surface
γ_x^0 and γ_θ^0	in-plane shearing strains of the reference surface
κ_x and κ_θ	change in the curvature of the reference surface
τ_x and τ_θ	torsion of the reference surface
μ_x^0 and μ_θ^0	the shearing strains
θ	circumferential co-ordinate
Φ	velocity potential
ω	natural frequency
ρ_s	density of the shell material
ρ_f	density of fluid, f_i for internal fluid and f_e for external fluid

List of matrices

$[A_1]_{(10\times10)}$, $[A_0]_{(6\times6)}$ and $[A_0']_{(4\times4)}$	defined by equations (11), (17) and (22)
$[B_1]_{(10\times10)}$	defined by equation (24)
$[C_f]$	damping matrix
$[k_f]$	stiffness matrix for a fluid finite element equation (51)
$[K_f]$	stiffness matrix for the whole fluid (53)
$[k_{1s}]$, $[k_{0s}]$ and $[k_{0s}']$	stiffness matrix for a shell finite element equations (26), (30) and (35)
$[K_s]$	stiffness matrix for the whole shell (53)
$[m_f]$	local mass matrix for a fluid finite element equation (51)
$[M_f]$	mass matrix for the whole fluid equation (53)
$[m_{1s}]$, $[m_{0s}]$ and $[m_{0s}']$	local mass matrix for a shell finite element equations (26), (30) and (34)
$[M_s]$	mass matrix for the whole shell equation (53)
$[N_1]$ and $[N_0]$	shape function matrices equations (12) and (19)
$[P]$	elasticity matrix equation (3)
$[Q_1]$, $[Q_0]$ and $[Q_0']$	defined by equations (23), (29) and (32)
$[R_1]$, $[R_0]$ and $[R_0']$	defined by equations (12), (16) and (21)
$[T]$	defined by equation (5)
$\{C\}$	vector for arbitrary constants (9)
$\{F\}$	force vector defined in equation (53)
$\{\delta_{1i}\}$, $\{\delta_{0i}\}$ and $\{\delta_{0i}'\}$	degrees of freedom at node **i** defined in equations (11), (18) and (21)
$\{\varepsilon_1\}$, $\{\varepsilon_0\}$and $\{\varepsilon_0'\}$	deformation vector equations (23), (29) and (32)
$\{\sigma_1\}$	stress vector defined in equation (24)